

AP. 638-728

IONOSPHERIC RESEARCH FROM SPACE VEHICLES

R. E. BOURDEAU

Space Sciences Division

NASA-Goddard Space Flight Center, Greenbelt, Maryland, U.S.A.

N 63 21280

CODE NONE

(Received January 12, 1963)

1. Introduction

Previous to the advent of artificial satellites, our knowledge of the ionosphere was limited principally to the interpretation of data from the classical ground-based ionosonde and a few rocket measurements of ionizing radiation, electron density and ion composition, all applicable to altitudes below the F2 peak. The early rocket results of SEDDON and JACKSON, which have been summarized by RATCLIFFE and WEEKES (1960), show that the lower ionosphere is characterized by an electron density which increases monotonically with altitude and thus that the term "layer" is an incorrect nomenclature for the D, E, and F regions. In more recent years, a wealth of data has been gathered on the temporal, spatial and energy distribution of the charged particles which for the ionosphere. This has been accomplished at previously relatively unexplored altitudes well above the F2 peak. Concurrently but unfortunately not simultaneously, measurements have been made of the time dependence of corpuscular, ultraviolet and X-radiation. The most serious observational gap is in the structure of the neutral atmosphere where the most significant contribution has been the computation of the neutral density parameter from satellite drag observations.

This paper compares the available interdisciplinary experimental data with theoretical models of the D, E, and F regions as well as the upper ionosphere, eventually selecting those models which best fit the spaceflight observations. Because a significant amount of low-energy charged particle data were obtained by direct sampling techniques and because this methodology is relatively new to ionospheric research, the paper contains brief discussions of the validity of some of these results as they are presented. Although the theoretical models of all ionospheric regions have been enhanced significantly by increased spaceflights, refinement and changes in these models await the next two major steps - the launching of satellites and rocket probes which are truly geophysical in nature and the correlation of such interdisciplinary measurements with data resulting from recent breakthroughs in ground-based observational methods.

2. The D Region Under Quiet Solar Conditions

The D region, situated between approximately 50 and 85 kilometers, is the lowest ionospheric subdivision where a significant number of free electrons are found. This

altitude interval is difficult to treat theoretically and experimentally because of the low charged particle concentrations, because the relatively high gas densities result in high electron collision frequencies, and because of the high probability of negative ion formation.

Spaceflight radiation observations made during the absence of solar flares show that the three most probable ionizing agents are cosmic, Lyman α (1215.7 Å) and X-radiations (2–8 Å). The most detailed theoretical analysis of D region formation has been performed by NICOLET and AIKIN (1960) using an expansion of the following equation of ionization:

$$q = (\alpha_d + b\alpha_i) n_+ n_e, \quad (1)$$

where q is the equivalent electron production rate, α_d is the loss coefficient for recombination of positive molecular ions with electrons, α_i the loss coefficient for recombination of positive with negative ions, b is the ratio of negative ions to electrons, and n_e and n_+ are the electron and positive ion concentrations, respectively. The cosmic and X-radiations act on molecular nitrogen and oxygen, the major neutral constituents, whereas Lyman α radiation acts on nitric oxide, a trace constituent. In their expansion of eq. (1), NICOLET and AIKIN produced a summation of the separate effects of the three ionizing sources and concluded that:

- (a) cosmic radiation is the most important ionizing agent at altitudes up to 70 km;
- (b) in the 70–85 km region, assuming an NO^+ recombination coefficient of $3 \times 10^{-9} \text{ cm}^3 \text{ sec}^{-1}$, a nitric oxide abundance of only 10^{-10} of the total neutral concentration is required to make X-rays (2–8 Å) unimportant to the formation of the D region under quiet solar conditions;
- (c) negative ions are unimportant above 70 km;
- (d) the ionization at altitudes between 85 and 100 km (base of the E region) is the result of X-rays (30–100 Å) and ultraviolet radiation (Lyman β and the Lyman continuum).

It is known principally from measurements made on the Greb satellite (KREPLIN, CHUBB and FRIEDMAN, 1962) and on the Orbiting Solar Observatory (LINDSAY, 1962) that the Lyman α energy flux ($3\text{--}6 \text{ erg cm}^{-2} \text{ sec}^{-1}$) is relatively constant with solar condition. The X-ray energy flux, however, is extremely variable. Consequently, it is possible that Lyman α and X-radiations alternate as the predominant ionizing agents of the normal upper D region. POPPOFF and WHITTEN (1962) have challenged the Lyman α hypothesis in attempting to account for the 70–85 km ionization entirely by X-radiation. However, they used energy flux values, which according to a recent review (FRIEDMAN, 1962), exceeds energies representative of a quiet sun even at the maximum of the solar cycle.

In this section it will be shown that to achieve agreement with spaceflight n_+ observations taken during quiet mid-solar cycle conditions, it is necessary to invoke the Lyman α hypothesis. Additionally it will be shown that to obtain consistency with ground-based measurements of electron density for similar conditions, existing D region formation theories must be considered incomplete. Specifically, it appears that

UNOL THE COPY

there is a tendency in most of the current models to underestimate the number of electrons lost in the various processes of negative ion formation.

It has been inferred in the previous discussion that care must be taken in comparing experimental results with theoretical models for the same solar condition. The extreme sensitivity of the X-ray energy flux to solar activity is demonstrated in Figure 1. It is

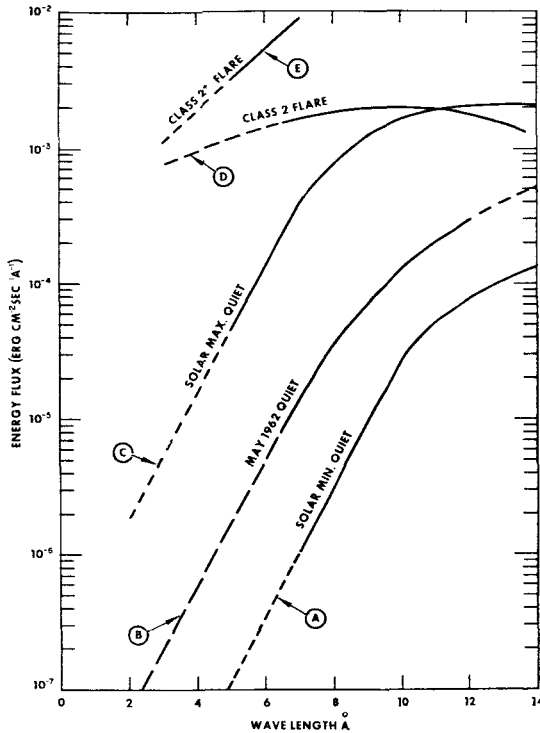


Fig. 1. The variability of solar X-ray emissions. Curves A, C and E are from FRIEDMAN (1962) Curves B and D are from POUNDS and WILLMORE (1962).

seen by a comparison of curves A and C (FRIEDMAN, 1962) that even in the absence of flares the intensity in the important wavelength region (2–8 Å) varies by two to three orders of magnitude during a complete solar cycle. The recent data (curve B) from the Ariel satellite (POUNDS and WILLMORE, 1962) correspond temporally to values used by NICOLET and AIKIN (1960) in computing their “quiet sun” model. The Ariel data also correspond most closely to the epoch of the solar cycle under which the few available D region charged particle density profiles have been obtained.

In Figure 2 are presented two theoretical electron density profiles (AIKIN, 1962a) which are intended by their contrast to illustrate the enhancement of n_e that should occur in the 70–85 km region if the NO concentration is 10^{-10} of the total concentration and if the negative ion abundance is that computed with the assumption that O_2^- is the principal negative ion. The alternative theoretical profiles were computed by using

X-ray energy fluxes approximately representative of curve B in Figure 1. The principal change from the original NICOLET-AIKIN model is that the values of α_d for O_2^+ and NO^+ were increased by a factor of ten. The O_2^+ coefficient is increased in the light of more recent laboratory investigations (KASNER, ROGERS and BIONDI, 1961) whereas in a succeeding section it is shown that an increase of α_d for NO^+ from 3×10^{-9} to

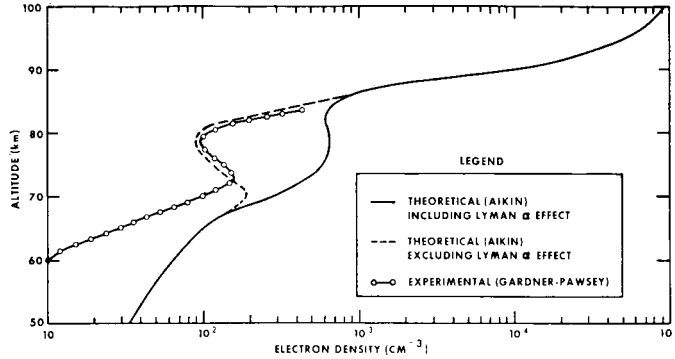


Fig. 2. Electron density profile of the quiet daytime D region at mid-latitudes for the period between solar maximum and solar minimum.

$3 \times 10^{-8} \text{ cm}^3 \text{ sec}^{-1}$ is more consistent with an effective recombination coefficient determined for the E region from diurnal variation observations.

To date, a reliable spaceflight method for measuring the low electron densities characteristic of the normal D region has not yet been developed. USSR data from a rocket-borne impedance probe for altitudes as low as 75 km have been published (KRASNUSKIN and KOLESNIKOV, 1962) but too recently for critical review. The lag in the development of rocket-borne electron density experiments is due primarily to the extremely low electron to neutral gas density ratio and the associated high collision frequencies. Because of this lag, it is necessary to resort primarily to electron density profiles obtained by ground-based methods.

In a recent review, RATCLIFFE and WEEKES (1960) conclude that D region electron density profiles obtained by ground-based methods should be treated with caution. According to this review, the most reliable of these profiles was obtained by GARDNER and PAWSEY (1953) using observations of weak backscatter echoes. The experimental data were obtained at a time when the values of the X-ray energy flux most likely were intermediate between those represented by curves A and B in Figure 1. The experimental data are plotted in Figure 2 for comparison with the alternative theoretical models. The valley of ionization which shows a minimum at about 78 km is typical of most of the few electron density profiles reported by other observers using ground-based techniques. BELROSE and BURKE (1961), for example, report a valley with the minimum located at 70 km, also using a backscatter method. There is a large difference between both theoretical ionization estimates and the experimental data at altitudes below 70 km. It has been concluded by others (BELROSE and BURKE, 1961) that

observational data by the backscatter method must be treated with caution in the lower D region because of simplifying assumptions in the APPLETON-HARTREE formula used to derive the experimental result. If the experimental data below 70 km are assumed correct, the low electron densities could be explained either by a theoretical overestimate of the effective cosmic ray electron production rate or an underestimate of the processes leading to the formation of negative ions or a combination of the two.

It is seen by a comparison of the experimental data with the two alternative theoretical models in Figure 2 that all of the ionization in the 70–85 km region could be explained from the X-ray effect alone as proposed by POPPOFF and WHITTEN without resort to the Lyman α hypothesis of NICOLET and AIKIN. However, a conclusion based on these few electron density data that the Lyman α radiation has a negligible effect on the formation of the D region would not be consistent with spaceflight observations of the positive ion characteristics, a discussion of which follows.

The first spaceflight measurements of D region ion parameters (BOURDEAU, WHIPPLE and CLARK, 1959) were obtained by use of a rocket version of a Gerdien condenser similar to that flown extensively on aircraft and balloons by workers in atmospheric electricity. This experiment measures ion conductivity (λ_+). In the altitude region where the number of free electrons is negligibly small, λ_+ can be estimated theoretically from

$$\lambda_+ = ek_+(q_+/\alpha_T)^{1/2}, \quad (2)$$

where e is the elementary charge, k_+ is the ionic mobility, q_+ is the rate of ion-pair production and α_T is THOMSON'S ion-ion volume recombination coefficient. The altitude dependence of k_+ and α_T are estimated from laboratory experiments. In the reported results, the altitude at which α_T can be extrapolated with confidence was overestimated. However, at altitudes up to 50 km where the use of α_T is appropriate, the experimental values of λ_+ are in good agreement with theoretical estimates based on Equation (2) in which q_+ is estimated from spaceflight observations of cosmic ray intensities. The experimental rocket values of λ_+ also are consistent with those obtained on balloons by other investigators. The importance of these agreements is that it lends some confidence to the theoretical conclusion (BOURDEAU *et al.*, 1959; ICHIMIYA, TOKAYAMA and AONO, 1959) that possible errors in the rocket experimental data associated with shock waves (thermal ionization, adiabatic compression etc.) are small, even at the relatively high D region gas pressures.

Positive ion densities now have been reported by SMITH (1961a) and AONO, HIRAO and MIYAZAKI (1961), each using a different method of computing n_+ from the observed current to an exposed electrode insulated from the rocket body. Their published values are compared in Figure 3 with a theoretical n_+ model (AIKIN, 1962a). Estimates of negative ion densities based principally on attachment and photodetachment processes are represented by the difference in the theoretical n_+ and n_e curves. Both sets of experimental data were obtained at a time when the values of the X-ray energy flux were most likely slightly larger than those represented by curve B in Figure 1.

It is seen from Figure 3 that the shape of the ion density profile experimentally obtained by SMITH is consistent with the shape of the theoretical n_+ curve and thus consistent with a hypothesis of three different ionization sources n_+ between 50 and 100 km, each predominating in a separate altitude region. However, it is seen also that the experimental values of n_+ are generally much higher than the theoretical values. The general excess of the experimental positive ion densities over the theoretical estimates may be interpreted as an altitude invariant error either in the experimental

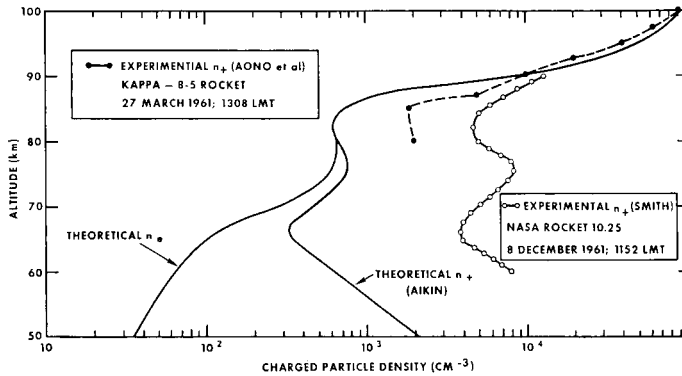


Fig. 3. Ion density profile of the quiet daytime D region at mid-latitudes for the period between solar maximum and solar minimum.

result or in one of the assumed theoretical parameters. It now will be shown that experimental uncertainties could account for the difference between the theoretical and experimental n_+ curves in Figure 3.

The results reported by SMITH (1961a) were obtained by the use of a standard asymmetric Langmuir probe in which the active electrode is the nose tip of the rocket. In the D region this Langmuir probe functions as a conductivity meter, the principle of operation being analogous to that of the exploratory Gerdien condenser experiment (BOURDEAU *et al.*, 1959). Positive ion current flowing from the ionosphere to the nose tip is measured as a function of a variable voltage applied between this electrode and the main rocket body. Values of λ_+ are computed by electrostatic theory from the slope of the volt-ampere curve when the active electrode is negative with respect to the ambient plasma. SMITH computed positive ion densities from the observed λ_+ according to the following simplified form of the pertinent electrostatic equation:

$$n_+ = (\lambda_+ m_+ v_+) / e^2, \quad (3)$$

where m_+ is the mean ionic mass and v_+ is the ion collision frequency. Laboratory investigations (LOEB, 1955) indicate that the simplifying assumptions leading to Equation (3) could result in uncertainties of a factor of two in the n_+ determination. SMITH

used values for v_+ contained in the 1959 ARDC model atmosphere which are probably uncertain by another factor of two (AIKIN, private communication). Consequently, the values of n_+ computed by SMITH could be uncertain by a factor of four just from the geophysical interpretation of the measured conductivity alone. This uncertainty is greater at altitudes above 80 km because the methods used to obtain λ_+ from the observed positive ion current are no longer valid when the ionic mean free path becomes large compared to the dimensions of the active electrode (BOURDEAU *et al.*, 1959).

Other possible errors in the measurement of D region ion characteristics are associated with aerodynamic effects (discussed previously) and the photocurrent effect. The latter effect represents the predominant criticism of ionospheric direct measurements techniques. For this reason, it is necessary to present the following arguments for a negligible photocurrent effect on the experimental n_+ results shown in Figure 3.

Because solar radiation can induce electron emission from rocket surfaces, an artificial electron current will flow from this electrode into the surrounding medium. This unwanted photocurrent is of the same polarity as the desired positive ion current. Values for the photocurrent density (j_p) of 2.3×10^{-9} amp cm^{-2} at an altitude of 200 km have been measured on a rocket (HINTEREGGER, DAMON and HALL, 1959) and of 5×10^{-9} amp cm^{-2} in the upper ionosphere on the Explorer VIII satellite (BOURDEAU, DONLEY, SERBU and WHIPPLE, 1961). The approximate agreement of the j_p values measured at such radically different altitudes should not be surprising because the most responsible solar radiation, occurring at wavelengths between 2000 and 3000 Å (HINTEREGGER *et al.*, 1959; ICHIMIYA *et al.*, 1959), is not significantly absorbed even in the D region.

The values of the perturbing photocurrent density listed above can be shown to be some two or three orders of magnitude larger than the ambient random ion current density flowing in a D region undisturbed by the presence of a rocket. However, the actual effect is dependent on the ratio a_+/a_p where a_+ is the effective ion collection area and a_p is that part of the active electrode's surface area which is exposed to the sun. This ratio is extremely difficult to obtain theoretically for the D region although orders of magnitude at large negative electrode potentials are indicated (ICHIMIYA *et al.*, 1959). It is possible by this mechanism then, to overcompensate in magnitude for the photocurrent effect. Confidence in this conclusion can be acquired by examination of observed D region volt-ampere curves. At negative electrode potentials, the current measured at the electrode is observed to be an order of magnitude larger than what would be expected from the product of j_p and a_p . Additionally even if the amplitude of the photocurrent was large, λ_+ is obtained from the slope of the volt-ampere curve at negative electrode potentials. This is a regime where the photocurrent is invariant with electrode potential. Hence it should not affect the measurement of the slope and thus the n_+ determination.

The n_+ data by AONO *et al.* (1961) shown in Figure 3 were obtained by measurement of the positive ion current to an effectively spherical electrode which was extended

along the major rocket axis. The term "effectively spherical" is used because although the electrode actually consists of two crossed rings, they are so arranged that the analysis for ions is as though the electrode were a solid sphere. The virtue of the crossed rings is that they present a much smaller target to solar radiation and consequently the experiment is even less sensitive to the photocurrent effect than the device used by SMITH.

A form of the conventional Langmuir probe theory applied to ions is used by the Japanese in computing n_+ from the experimental volt-ampere curves. The general agreement of their published n_+ values with an independent simultaneous measurement of n_e in the E region speaks well for the validity of their application of this theory at least for the simple case of no collisions in the plasma sheath surrounding the probe. However, their published data show slightly larger electron than ion concentrations in some portions of the E region which are in turn indicative of second-order errors even for the simple case. The validity of Langmuir probe theory becomes more uncertain at D region altitudes where multiple collisions within the sheath complicate the application of the conventional Langmuir probe theory. Thus, for different reasons associated with the interpretation of the observed volt-ampere curves the largest uncertainty in both sets of experimental data shown in Figure 3 can be expected between 80 and 90 km. It would not be surprising, therefore, if the same factor of 4 in the difference between the experimental data in the 80–85 km region were obtained even under identical solar conditions.

It generally is concluded by this author that the uncertainties in the D region experimental n_+ values could be large enough to adjust to the theoretical n_+ estimates of AIKIN (1962a). On the other hand, it is unlikely that the experimental inadequacies are sufficient to adjust rocket observations of n_+ to the experimental electron density values shown in Figure 2, thus suggesting a much higher negative ion abundance than estimated theoretically by NICOLET and AIKIN (1960) and by WHITTEN and POPPOFF (1961). The high negative ion abundance is more in accordance with the theoretical model of MOLER (1960). The suggestion of high negative ion densities also is consistent with values computed from the original experimental conductivity data by WHIPPLE (1960) who suggests that dust particles believed responsible for noctilucent cloud formation at high latitudes could provide an important recombination surface for charged particles in the D region. The simultaneous measurements of electron and positive ion densities made by AONO *et al.* (1961) show somewhat larger n_+ values in the 95 km region again suggesting a large negative ion abundance at the lower D region altitudes where their formation is even more likely.

The few data that are available support a tentative conclusion of ionization of the lower and upper D regions by cosmic and Lyman α radiation, respectively, during conditions of a quiet sun at the middle of the solar cycle. A firm conclusion awaits more accurate measurements of electron and ion densities obtained simultaneously with observations of the pertinent energy fluxes of the ionizing sources. Just as important is the need for improved knowledge of the pertinent reaction rates and of the number density of the trace neutral constituents.

3. The D Region During Disturbed Solar Conditions

During periods of high solar activity, the D region is characterized by enhanced ionization with associated electromagnetic wave attenuation strong enough to produce radio blackouts. There are many phenomena associated with solar flares which increase the normal D region electron densities by up to two orders of magnitude. A comparison of the amount of enhanced ionization for different types of solar flare events is made with the NICOLET-AIKIN quiet sun model (curve A) in Figure 4.

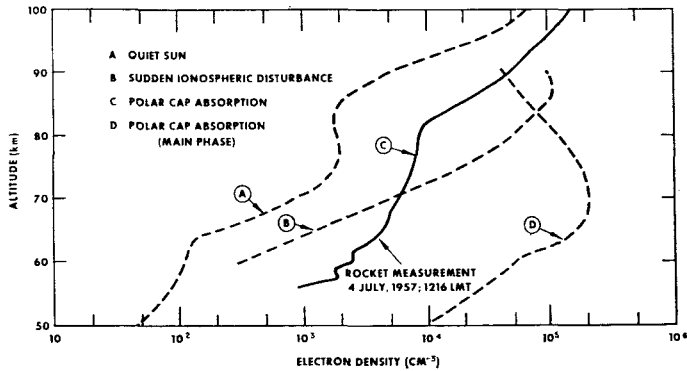


Fig. 4. Comparison of the D region under quiet and disturbed solar conditions.

Simultaneously with the appearance of the flare, radio absorption is observed in the D region on the sunlit side of the earth for periods lasting up to approximately one hour. This particular phenomenon is called a Sudden Ionospheric Disturbance. CHUBB, FRIEDMAN and KREPLIN (1960) made rocket flights into such events and observed abnormally high X-ray fluxes at extremely low D region altitudes. These observations have been used in Equation (1) by NICOLET and AIKIN (1960) to calculate an S.I.D. electron density profile (curve B of Figure 4). Here, the influences of cosmic and Lyman α radiation become minor, the secondary layer in the 70–85 km region disappears, and the profile is characterized by overall enhancement and a monotonically increasing electron density. The S.I.D. profile does not include the contribution of radiation responsible for the formation of the E region. Observations from the Greb satellite show that whenever the X-ray flux at wavelengths shorter than 8Å exceeds a critical value of 2×10^{-3} erg cm⁻² sec⁻¹, radio fadeouts at short wavelengths and other sudden ionospheric disturbances occur (FRIEDMAN, 1962). It is seen from curves D and E in Figure 1 that this high flux value generally would be characteristic of flares stronger than importance 2.

A second type of ionospheric storm predominates at night and is associated with active aurorae and magnetic disturbances. It generally is accepted that the ionizing agents are energetic particles comprising corpuscular emission from the sun, a belief founded on the observation that D region absorption occurs some 21 hours after the appearance of a flare, an interval corresponding to the sun-earth transit time for these

particles. During the storm, D region electron densities increase to values high enough that echoes are observed on ionosondes. "Layers" appear at 90 km during weak geomagnetic activity and as low as 70 km for the more active events.

A third type of disturbance occurs only at auroral latitudes. These phenomena, called Polar Cap Absorption (PCA) events, are produced by energetic protons emitted from the sun during certain flares. Here echoes are observed from ionosondes at altitudes as low as 60 km. The phenomenon has been the subject of considerable

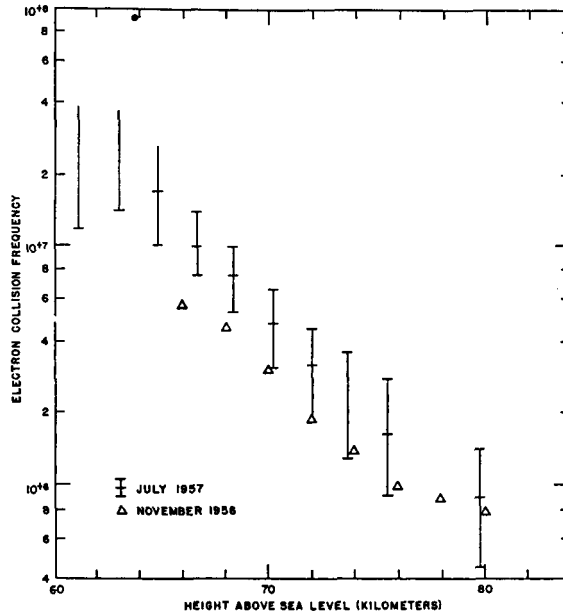


Fig. 5. Rocket measurement (KANE, 1960) of the altitude dependence of electron collision frequency.

study during the past few years. Most recently, MAEHLUM and O'BRIEN (1962) have proposed a semi-quantitative time history of the D region electron density profile during a PCA by inserting proton fluxes observed on the Injun satellite as a source function in the conventional equation of ionization. One of these profiles (curve D of Figure 4) coincides with the peak of 27.6 Mc cosmic radio noise absorption (17 db) observed at College, Alaska. Like the NICOLET-AIKIN model for an S.I.D., curve D does not contain the contribution due to solar radiation. Inclusion of solar radiation should modify the result in the base of the E region (above 80 km). JACKSON and KANE (1959) used a rocket-borne radio propagation experiment to measure a D region electron density profile (curve C of Figure 4) during a less active phase of a PCA event (3 db absorption at 30 Mc). This profile compares favorably in shape but is generally less enhanced than that proposed by MAEHLUM and O'BRIEN for an interval when the observed radio absorption also was 3 db. If, as the evidence presented in the previous section indicates, there is a higher D region negative ion abundance than is generally

accepted, then the three dashed curves in Figure 4 could represent overestimates of the electron density.

The strong absorption of radio waves in the D region is made possible by the high electron collision frequencies characteristic of this altitude interval. KANE, (1959, 1960) has derived an electron collision frequency model from measurements of the difference in the absorption of ordinary and extraordinary radio propagation modes. His data which represent the best available rocket measurements of the altitude dependence of this important D region parameter are presented in Figure 5. They were obtained on two separate rocket flights flown during auroral absorption events.

4. The Ion Content of the Lower Ionosphere

To a high degree of probability, the predominant ionizing sources of the E and F regions for quiet solar conditions at mid-latitudes are solar ultraviolet and X-ray radiations. It is possible to compute the rate at which different ion species are formed from a knowledge of the altitude dependence of the number of photons incident at each wavelength, of the densities of the individual neutral constituents and of the absorption and ionization cross sections of these constituents. There are available some altitude profiles of the photon fluxes as a function of wavelength but only for limited conditions. Early results from rocket-borne neutral gas spectrometers reported to date are extremely controversial. The validity of these results is questioned justifiably because recombination effects within the instruments distort the gas under study from its ambient condition. Thus most model atmospheres do not depend on experimental observations but rather are derived from the hydrostatic laws using an assumption for the critical altitude of diffusive separation. Our knowledge of the important cross sections also must be considered incomplete.

The most recent estimate of the altitude dependence of the rate at which various ions are produced was made by WATANABE and HINTEREGGER (1962) using solar radiation data obtained by HINTEREGGER under quiet solar conditions at mid-latitudes. The rates for the ions formed in greatest abundance (N_2^+ , O_2^+ , O^+) are illustrated in the left-hand side of Figure 6. WATANABE and HINTEREGGER hasten to point out that these curves must be considered suggestive rather than quantitative principally because of the uncertainty in our knowledge of the neutral atmospheric composition. Some adjustment of these rates already are indicated from very recent neutral gas spectrometer results (SCHAEFFER, 1963). These results were obtained by use of a spectrometer which overcomes the inadequacies of the early devices by ionizing the gas under study before its entry into the instrument's analyzer section. The results show a larger ratio of atomic to molecular oxygen than that used to obtain the ion production rates shown in Figure 6.

Some indication of the solar radiation responsible for the production of various ionospheric regions can be made by comparing the inferred production rates of the individual ionic species with rocket-borne ion spectrometer results. Early rocket flights (JOHNSON, MEADOWS and HOLMES, 1958) of a radio-frequency mass spectro-

meter made in the auroral zone showed that the diatomic ions, O_2^+ and NO^+ , predominate below 200 km and that O^+ is the principal ion found above this altitude. These results have been confirmed by ISTOMIN (1960) and by TAYLOR and BRINTON (1961). The rocket data of TAYLOR and BRINTON shown in the right hand side of Figure 6 are selected for comparison with the production rates because they were obtained for latitude and temporal conditions most closely representing those under

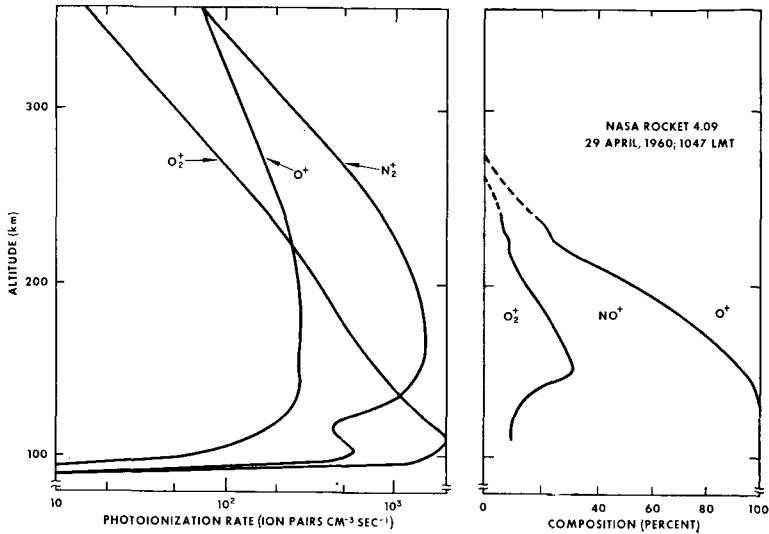


Fig. 6. Comparison of the production rate and the actual abundance of ions in the lower ionosphere.

which the photon fluxes used in estimating the photoionization rates were obtained. It is seen in the comparison that although the diatomic nitrogen ions are expected to be produced in great quantities, the spectrometer results show that they exist only as extremely minor charged constituents. The most likely reason is that N_2^+ ions dissociatively recombine ($N_2^+ + e \rightarrow N' + N'$) at a very rapid rate as demonstrated by FAIRE and CHAMPION (1959).

It was inferred in the previous section that there is general acceptance that X-radiation at wavelengths longer than 10 Å and ultraviolet radiation (Lyman β and the Lyman continuum) are responsible for the base of the E region (85–100 km). There remain two schools of thought for the formation of the remainder of the E region: (a) general ionization of air by soft X-rays (VEGARD, 1958; HULBURT, 1958; BATES, 1956; FRIEDMAN, 1959) and (b) photoionization of O_2 by solar radiation in the wavelength region between 800 and 1026 Å (WULF and DEMING, 1938; NICOLET, 1945; WATANABE, MARMO and PRESSMAN, 1945). On the basis of more accurate solar radiation data, WATANABE and HINTEREGGER (1962) strongly support ionization of the 100–120 km region by direct production of O_2^+ from ultraviolet radiation at wavelengths between 911–1027 Å. Part of this conclusion is based on the agreement

between experimentally observed E region electron densities and those computed from the conventional ionization equation under quasi-equilibrium conditions:

$$n_e = (q/\alpha_a)^{1/2}, \quad (4)$$

where q is the photoionization rate for O_2^+ computed from the observed ultraviolet photon fluxes.

However, there are two sets of recent experimental evidence which indicate that WATANABE and HINTEREGGER overestimated the electron density produced in the 100–120 km region by ultraviolet radiation. Firstly, the recent rocket neutral gas spectrometer results indicate that the O_2 concentration and thus the O_2^+ production rate have been overestimated. Secondly, WATANABE and HINTEREGGER used a value for the O_2^+ recombination coefficient taken from NICOLET and AIKIN (1960) of $3 \times 10^{-8} \text{ cm}^3 \text{ sec}^{-1}$ which as discussed in the previous section appears from more recent laboratory work to be an order of magnitude too low.

A third set of experimental data which also tends to favor X-radiation as the more important agent for E region formation involves the rocket ion spectrometer data shown in Figure 6. The diatomic ion NO^+ is observed to be predominant at E region altitudes. Its existence can best be explained (AIKIN, 1962b) by ion-atom interchange involving the O^+ ion ($O^+ + N_2 \rightarrow NO^+ + N$). The ultraviolet radiation (911–1027 Å) observed to penetrate below 120 km (HINTEREGGER and WATANABE, 1962) lies in a range above the ionization threshold for O^+ . Consequently to be consistent with the rocket ion spectrometer observation that NO^+ is the predominant E region ion, the ultraviolet hypothesis requires a reaction leading to NO^+ formation involving O_2^+ , a reaction not considered by HINTEREGGER and WATANABE. Parenthetically, it is difficult to dispute the correctness of the observed ratio NO^+/O_2^+ from an experimental point of view since the principal corrections which must be made to the measured ion spectrometer target currents involve the effects of vehicle motion and of electric fields due to the attracting vehicle potential. Both of these effects are expected to be nearly the same for ions of approximately the same mass. Hence, the measurement of their relative abundance should be reasonably accurate. As HINTEREGGER and WATANABE (1962) demonstrate, the ion spectrometer measurement of the increasing importance of O^+ with altitude leading to its predominance above 200 km is explained adequately by the simultaneously increasing role of extreme ultraviolet radiation in the wavelength region between 280 and 911 Å.

5. The Diurnal and Anomalous Behavior of the E Region

The altitudes generally assigned to the E region lie between approximately 85 and 140 km. The most accurate rocket method of daytime electron density determination for this altitude region remains the SEDDON two-frequency radio-propagation experiment. Results from this experiment early demonstrated that the lower ionosphere is not characterized by discrete layers but rather that the electron density increases monotonically with altitude and thus that the F region is a continuation of the upper E

region. Until recently, there have been no detailed observations of nighttime E region ionization because neither this rocket-borne experiment nor ground-based ionosondes are sensitive enough. Now the introduction of low energy plasma probes into space-flight studies of the ionosphere permits our first insight into the diurnal characteristics of the E region.

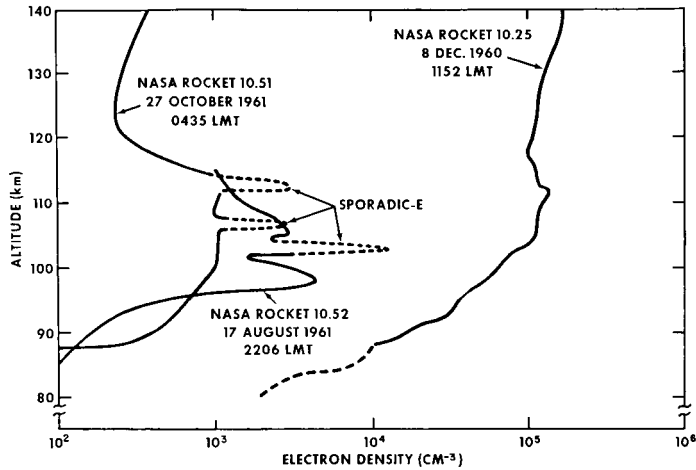


Fig. 7. Rocket measurements of the diurnal and anomalous behavior of the E region.

Electron density values reported from one daytime and two nighttime rocket launchings of an asymmetric Langmuir probe (SMITH, 1961a; SMITH, 1961b) are presented in Figure 7. It is seen that the electron density in the lower portion of the nighttime E region is found to be $3 \times 10^3 \text{ cm}^{-3}$ at approximately 22h LMT and $1 \times 10^3 \text{ cm}^{-3}$ near sunrise, both about two orders of magnitude less than typical daytime values. SMITH (1961b) has used this observed diurnal variation to compute an effective E region recombination coefficient of $2 \times 10^{-8} \text{ cm}^3 \text{ sec}^{-1}$, which is perhaps mostly representative of the observed predominant ion, NO^+ . In the view of this author, this value should be considered approximate, firstly because of possible second-order errors in computing absolute values of n_e from the observed volt-ampere curves and secondly because it is assumed that there is no nighttime ionization source. It is tempting from the observation of deep ionization valleys characteristic of the upper nighttime E region profiles shown in Figure 7 to suggest that the ledges in the lower E region result from observed scattering (DONAHUE, 1962) of ultraviolet radiation in the night sky.

The other significant data contained in Figure 7 are associated with the measurement of the ionization characteristics of the sporadic-E layer (E_s), which on an ionosonde is characterized by echo reflection from a constant virtual height. The statistical occurrence of the E_s phenomenon from ionosonde data has been the subject of considerable study, yet the causes of sporadic-E layers remain topics for speculation.

Early rocket observations of daytime E_s ionization were obtained by SEDDON and JACKSON (1958).

Two types of E_s ionization, differing in horizontal dimensions are contained in Figure 7. It is seen that the electron density observed in the sporadic-E layer (102 km) on the 17 August flight represents an enhancement of about a factor of four above the average lower E region value. The thickness of the layer measured at half the peak electron density was 450 meters. The layer was detected at precisely the same altitude on both the ascent and descent portions of the rocket trajectory, indicating a horizontal dimension greater than 72 km. Similar characteristics were observed at an altitude of 112 km on the 27 October flight. It has been suggested (WHITEHEAD, 1960) that E_s ionization with these characteristics results from re-distribution of electrons by wind shear in the presence of a geomagnetic field, rather than local changes in electron production or loss.

On the 27 October flight, another type of E_s ionization was observed. One such electron density peak is shown at an altitude of approximately 108 km in Figure 7. A larger number of such peaks than indicated in Figure 7 were observed with no correlation between the ascent and descent portions of the trajectory. The small horizontal dimensions lead SMITH (1961b) to support current theories that some types of E_s ionization result from meteor trails.

It can be said that there is insufficient evidence to support conclusively any current theories to account for E_s ionization. Such evidence will come from planned correlative experiments performed simultaneously with charged particle density measurements. The rocket data are, however, serving to define the dimensions and ionization characteristics of sporadic-E layers. One of the most detailed altitude definition of the E_s ionization reported to this author was obtained by BOYD (private communication) from a daytime ion density profile on December 6, 1961. His observation of a depth of just under one kilometer and an ionization enhancement of about a factor of 3 is consistent with the results shown in Figure 7.

In addition to the measurement of electron density the asymmetric Langmuir probe is designed to provide data on the electron temperature, T_e . For the same rocket flight from which the daytime electron density profile illustrated in Figure 7 was obtained, SMITH (1961a) reported electron temperature values of 1400° K with little altitude variation between 100 km and the apogee altitude of 155 km. The disagreement of these T_e values with current hypotheses for this altitude region and with the results of other rocket experiments made under quiet daytime conditions justifiably has raised some questions as to the validity of the electron density results. There are two possible explanations for the differences. The first, geophysical in nature, is that this particular rocket flight took place within twenty-four hours of a geomagnetic disturbance. Current theoretical concepts of expected differences between the electron and neutral gas temperatures do not include the extreme variability of X-ray fluxes which perhaps could account for the high electron temperature. On the other hand it is just as likely, from this author's point of view, that the high electron temperatures result from simplifying assumptions used in deriving T_e from the observed volt-

ampere curves. Specifically, n_e and T_e both are derived from the volt-ampere curve after unwanted photocurrent and positive ion currents are subtracted out. T_e is computed from the slope of the corrected curve at negative collector potentials and is sensitive to the accuracy of the correction. The electron density, on the other hand, is computed from the current observed at a distinct discontinuity in the curve where the collector is at plasma potential. At this point the electron current is more than an order of magnitude higher than the unwanted current and hence the derivation of n_e is insensitive to the assumed corrections. Thus the errors in deriving n_e are small enough to have little effect on the important conclusions from Figure 7 relative to (a) the magnitude of the diurnal variation of n_e in the lower E region, (b) the observation of a deep ionization valley in the upper E region at night, and (c) the major characteristics of sporadic-E ionization.

6. The Formation of the F2 Peak

The altitudes generally assigned to the F region lie between 140 km and the altitude at which O^+ ceases to be the predominant ion. This region contains the altitude (F2 peak) of the maximum electron density found in the ionosphere. It was not until very recent years that significant experimental data on the characteristics of the upper F region were obtained. Local charged particle density measurements now have been made on satellites using ion traps (KRASSOVSKY, 1959; BOURDEAU, 1961) and rf impedance probes (BOURDEAU and BAUER, 1962; ULWICK and PFISTER, 1962; SAYERS, ROTHWELL and WAGER, 1962).

More meaningful to the physics of the F region have been experimental measurements of the charged particle density distribution with altitude where latitudinal and temporal variations can be neglected. Such profiles have been obtained from ground-based experiments (VAN ZANDT and BOWLES, 1960), rocket-borne radio propagation experiments (BERNING, 1960; JACKSON and BAUER, 1961; KNECHT and RUSSELL, 1962) and ion traps (HANSON and MCKIBBIN, 1961; HANSON, 1962a). These investigators all have concluded from their observations of an electron density distribution with a practically constant logarithmic slope taken over a few hundred kilometers that the upper ionosphere can be represented as an isothermal medium in diffusive equilibrium.

The most favored theory of the formation of the F2 peak at mid-latitudes under quiet solar conditions can be illustrated by comparing these charged particle density profiles with the altitude dependence of electron production rate inferred by WATANABE and HINTEREGGER (1962). Such a comparison is made in Figure 8, using the electron density profile obtained by JACKSON and BAUER (1961) with a rocket-borne cw radio propagation experiment. It has been recognized that, as illustrated, the altitude of the F2 peak lies considerably above that of the maximum electron production rate. This is best explained from the following form of the continuity equation corresponding to quasi-equilibrium:

$$q = \beta n_e + \frac{d}{dz} (n_e W_d), \quad (5)$$

where β represents an attachment - like loss coefficient, z is the altitude and W_d serves to define changes in electron density by vertical motion or diffusion. In the region up to the F2 peak, βn_e predominates over the diffusion term and because it decreases more rapidly with altitude than the electron production rate, q , n_e increases with altitude up to its maximum value. Near the F2 peak, the diffusion term becomes larger than βn_e

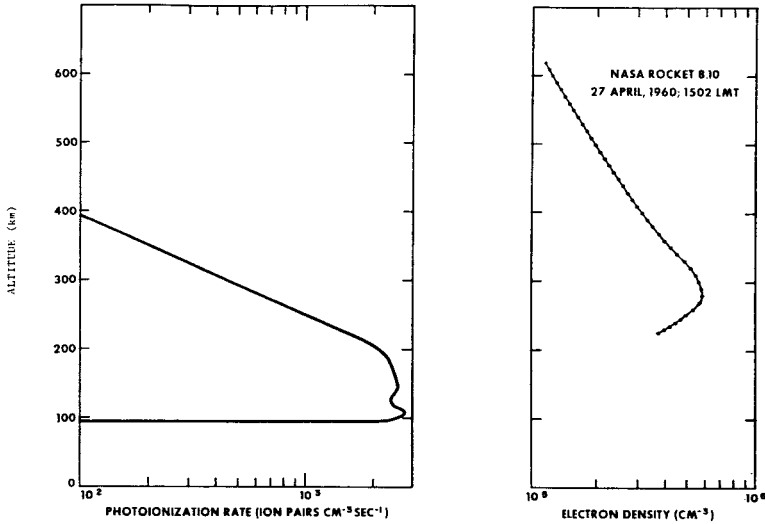


Fig. 8. Comparison of the altitude dependence of electron production rate and electron density, illustrating the formation of the F2 peak.

and the electron density begins to decrease. The diffusion mechanism is caused by gravitational forces acting upon the ions which, by coulomb attraction, cause the electrons to diffuse downward. At altitudes well above the F2 peak where q and βn_e in Equation (5) can be considered negligible, the electron density distribution is given by the diffusive equilibrium equation:

$$\frac{d(\ln n_e)}{dz} = \frac{m+g}{k(T_e + T_i)}, \tag{6}$$

where g is the acceleration of gravity, k is the Boltzmann constant, and T_e and T_i are the electron and ion temperatures. This most favored model of the formation of the F2 peak perhaps requires some modification near the geomagnetic equator where because of the existence of a horizontal magnetic field, diffusion cannot readily produce vertical movements.

Many empirical attempts have been made to solve the continuity equation, Equation (5), by making assumptions about the nature of the vertical movement, the production term, q , and the loss coefficient, β , and comparing the calculated results with experimental ones. Principally because of the numerous variables involved, these models vary considerably - from attempts to explain the F2 peak without diffusion

(SAGALYN and SMIDDY, 1963) to agreement with the most-favored theory discussed above. As an example of the latter case, CHANDRA (1963) finds that the attachment-loss and diffusion terms are of equal importance near the F2 peak by a computation involving n_e and q from Figure 8 and a loss coefficient behavior given by RATCLIFFE, SCHMERLING, SETTY and THOMAS (1956).

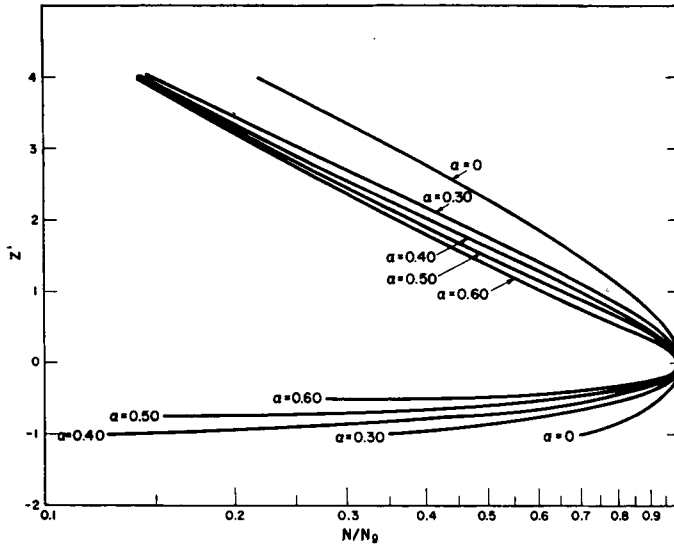


Fig. 9. Empirical model (CHANDRA, 1963) of the shape of the F2 peak.

Other empirical models have been developed to describe the electron density distribution of the F region from a knowledge of the electron density and an arbitrarily-defined scale height both measured at the F2 peak. These models vary in complexity from the use of a simple CHAPMAN distribution with a constant scale height (WRIGHT, 1960) to a variable scale height (YONEZAWA and TAKAHASHI, 1960) and finally a variable scale height gradient (CHANDRA, 1963). The latter model, applicable to an isothermal region where O^+ dominates, provides good empirical agreement with all available mid-latitude profiles attempted at height ranges between 100 km below the peak to about 700 km. CHANDRA's empirical model is illustrated in Figure 9 where the abscissa (N/N_0) is the ratio of the electron density at a given altitude to its value at the F2 peak, and the ordinate z' is given by

$$z' = (h-h_m)/H_0, \quad (7)$$

where $(h-h_m)$ is the height measured from the F2 peak and H_0 is the scale height corresponding to atomic oxygen. The parameter α is a measure of the departure from a simple CHAPMAN distribution and is given by

$$\alpha = (H_0-H_m)/H_0, \quad (8)$$

where H_m is the "scale height" at the F2 peak. CHANDRA finds that the "scale height"

values computed from available electron density profiles correspond closely to neutral gas scale heights taken from the 1961 COSPAR International Reference Atmosphere.

7. The Helium Ion Layer and the Protonosphere

For a given value at a reference altitude, the upper ionosphere electron density which is given by Equation (6) will be governed by the mean ionic mass and the sum of the electron and ion temperatures. Charged-particle density profiles obtained at mid-latitudes under quiet solar conditions predominantly show that $T_e + T_i$ is practically constant at altitudes above 450 km. Consequently, changes in scale height of the electron-ion gas in the upper ionosphere predominantly reflect the transition from one ion species to a lighter one. It will be shown in this section that early concepts of an upper ionosphere characterized only by O^+ and H^+ ions and by a reasonably constant transition altitude now should be discarded in favor of a three-constituent medium having an intervening helium ion layer with a thickness which varies considerably with the atmospheric temperature.

Drag observations on the Echo satellite led NICOLET (1961) to first suggest that helium should be considered an important constituent of the upper ionosphere. The first experimental evidences for the existence of helium ions in the upper ionosphere were obtained independently by an indirect method (HANSON, 1962a) and by direct measurement (BOURDEAU, DONLEY, WHIPPLE and BAUER, 1962). HANSON, working from an ion density profile obtained by HALE (1961) concluded that the thickness of the helium ion layer is of the order of 2000 km, extending from 1200 to about 3400 km, and that the measured scale height for helium ions corresponds to an atmospheric temperature of 1600° K. From the observed helium ion content (10^{12} ions/cm²) and an assumed rate of ionization, HANSON computed an equilibrium time for helium ions of about three days. He thus postulated that there should be no large diurnal variations

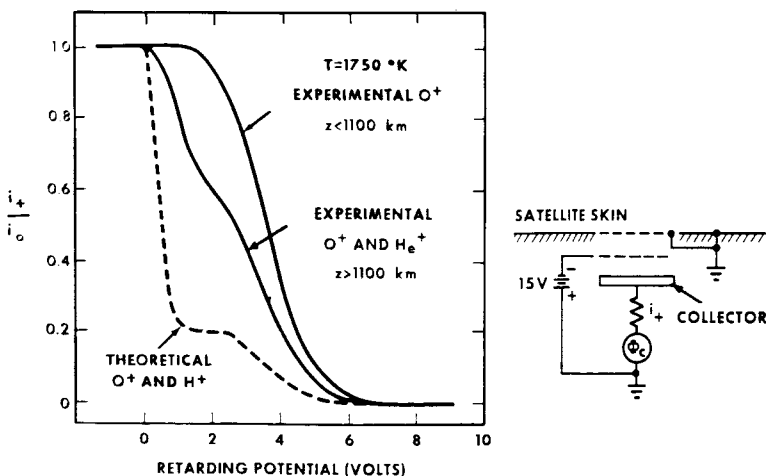


Fig. 10. Direct detection of helium ions from the Explorer VIII retarding potential experiment.

in the helium ion layer. This conclusion has not been corroborated by other experimental observations and by the theoretical work of BAUER (1962, 1963).

The Explorer VIII results (BOURDEAU *et al.*, 1962) relative to direct detection of helium ions are summarized in Figure 10. This retarding potential experiment differs only in geometry from the device used by USSR investigators (KRASSOVSKY, 1959) on Sputnik III. The sensor consists of three electrodes arranged in planar concentric geometry. The inner grid is biased negatively so that the collector is responsive only to the flow of positive ions from the ionosphere. Because the satellite velocity largely exceeds the thermal velocity of the ions, the latter have a kinetic energy relative to the spacecraft in proportion to their mass. In accordance with an expression given by WHIPPLE (1959) the resulting volt-ampere curve, illustrated in Figure 10, will be characterized by an inflection point for a mixture of O^+ and He^+ and by a plateau for a mixture of O^+ and H^+ . The abscissa of the volt-ampere curve is the total retarding potential given by the sum of the satellite and applied collector (ϕ_c) potentials while the ordinate is the ratio of the ion current at a given retarding potential to its value at zero potential. Planar ion traps have a good history for positive ion density determination but generally yield too high an ion temperature (HANSON and MCKIBBIN, 1961; BOURDEAU *et al.*, 1961), possibly due to an enhancement in the normal component of the particle energy caused by non-planar sheath geometry (HINTEREGGER, private communication). This factor is not considered in WHIPPLE's theoretical relationship. However, because of the relative insensitivity of the shape of the volt-ampere curve to ion temperature, the ability to determine ion composition is not altered significantly. For daytime conditions, the Explorer VIII observations during the active life of the satellite (November–December, 1960) were that O^+ predominated below 1100 km and that He^+ was the principal ion from 1100 km to the maximum altitude (1600 km) of the measurements. Unfavorable vehicle orientation prevented valid measurements for nighttime conditions and at altitudes above 1600 km.

Subsequent to the reporting of the first experimental evidence for the importance of upper atmosphere helium ions, BAUER (1962) theoretically showed that the thickness of the layer would change with atmospheric temperature even for the simple case when the relative concentrations are invariant at a reference altitude. Assuming that the ionic species are distributed according to diffusive equilibrium (DUNGEY, 1955; MANGE, 1960), the geopotential altitude (h'_{ij}) at which two ionic species have equal concentrations has been given by BAUER (1962) as

$$h'_{ij} - h'_o = H_{ij} \ln n_{ij}, \quad (9)$$

where h'_o is the geopotential altitude at which the concentrations of these ions are in the ratio n_{ij} , and where

$$H_{ij} = kT/(m_i - m_j)g_o, \quad (10)$$

T being the atmospheric temperature and g_o the acceleration of gravity at the earth's surface.

BAUER (1963) has proposed a more detailed theoretical model for the thickness of the helium ion layer as a function of atmospheric temperature by considering the case

where the relative concentrations of the three principal constituents vary at the reference altitude. He points out that the relative concentrations at a given altitude should vary with temperature in the same proportion as the ratio of the corresponding neutral constituents. Using the temperature dependent escape rate given for hydrogen (BATES and PATTERSON, 1961) and for both hydrogen and helium (NICOLET and KOCKARTS, 1962) and Equations (9) and (10), he computed two transition altitudes as a function of atmospheric temperature, a lower transition altitudes where O^+ and He^+ ions have equal concentrations and an upper transition altitude where He^+ and H^+ are

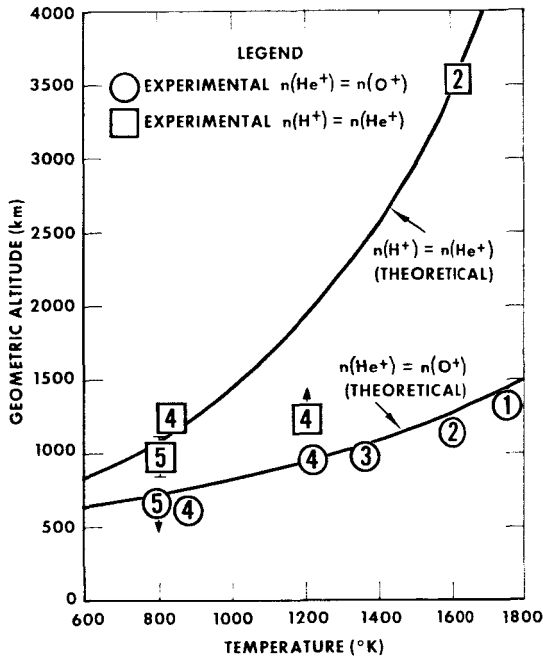


Fig. 11. Comparison of experimental measurement with theoretically-obtained model (BAUER, 1963) of ion transition altitude as a function of atmospheric temperature.

of the same density. These curves are shown to be in reasonably good agreement with experimental observations in Figure 11. The circles in Figure 11 refer to observed altitudes at which $n(He^+) = n(O^+)$ while the squares represent measured altitudes at which $n(He^+) = n(H^+)$. The corresponding temperatures were obtained on the same spacecraft and represent either direct measurements of T_e or T_i or values of $(T_e + T_i)/2$ computed from the observed electron-ion scale height. The abscissa, then, corresponds to the neutral gas temperature only if it is assumed that the electron, ion and neutral gas temperatures all are in equilibrium at the altitudes indicated.

Experimental points 1 and 2 are taken from BOURDEAU *et al.* (1962) and HANSON (1962a), respectively. Experimental points 4 represent the first preliminary results from the Ariel satellite (WILLMORE, BOYD and BOWEN, 1962). The Ariel investigators found that under daytime conditions helium ions predominated at altitudes between

950 km and to at least 1200 km, the satellite apogee. For a nighttime condition, it was found that the base of the helium ion layer was below 650 km and that hydrogen ions dominated at 1200 km.

The Ariel experiment is based on the same principle as that of the Sputnik III and Explorer VIII retarding potential experiments and yet, in the opinion of this author, represents a major advance in the development of ion spectrometers for upper ionospheric studies. Because of the spherical geometry used, it should not be as sensitive to the direction of the ion trajectory and thus provides valid measurements of ion temperature in contrast to the planar ion traps. Additionally, the Ariel investigators set up the experiment so that the second derivative of the volt-ampere curve is telemetered directly. This reduces the effects of slowly-varying vehicle potentials and other ion sheath parameters. These two basic differences make for a higher ion composition resolution than is possible with the Sputnik III and Explorer VIII ion traps.

The Ariel satellite observations are extremely important in explaining the failure (ULWICK and PFISTER, 1962) to detect He^+ ions from scale-height changes in nighttime electron density profiles. As Bauer correctly points out, the thickness of the helium ion layer is smaller than a helium ion height at low temperatures characteristic of a nighttime profile. As a result, the detection by indirect methods requires an extremely accurate charged-particle density profile. The detection of this layer is expected to become even more difficult as we approach the year of minimum solar activity.

Experimental points 3 and 5 in Figure 11 were obtained by the indirect method from electron and ion density profiles obtained on Scout rockets. These data are presented in the succeeding section to illustrate the diurnal variation of electron density in the extreme upper ionosphere.

8. The Diurnal Variation of Electron Density in the Upper Ionosphere

The diurnal variation of electron density in the upper ionosphere is a complicated function of the electron density at and altitude of the F2 peak, the atmospheric temperature, and the extremely variable heights of the two ion transition altitudes. This variability can be illustrated by comparison of two charged particle density profiles taken near the diurnal maximum and minimum during this portion of the solar cycle. That representative of diurnal maximum conditions is illustrated in Figure 12. The circled points are electron density values obtained by BAUER and JACKSON (1962) from FARADAY rotation observations at 72 Mc. The left-hand ordinate is geopotential altitude which takes into account the altitude dependence of the acceleration of gravity while the right-hand ordinate is the true or geometric altitude. HANSON (1962a) and BAUER (1962) have developed expressions based on an expansion of Equation (6) for the electron density distribution in a multi-constituent isothermal medium in diffusive equilibrium. These expressions suppose a given ratio of the concentrations of the pertinent ions at a reference altitude. In Figure 12, two such theoretical curves (BAUER, 1962) are shown to illustrate the dependence of the electron density distribution on the ionic constituents. It can be seen that the circled

points are more consistent with a theoretical curve for a mixture of O^+ and He^+ (solid line) than a mixture of O^+ and H^+ (dashed curve).

The charged particle density profile obtained near diurnal minimum conditions is illustrated in Figure 13. Both ion density (DONLEY, 1963) and electron density were measured. In the latter case, data were obtained only to a geopotential altitude of

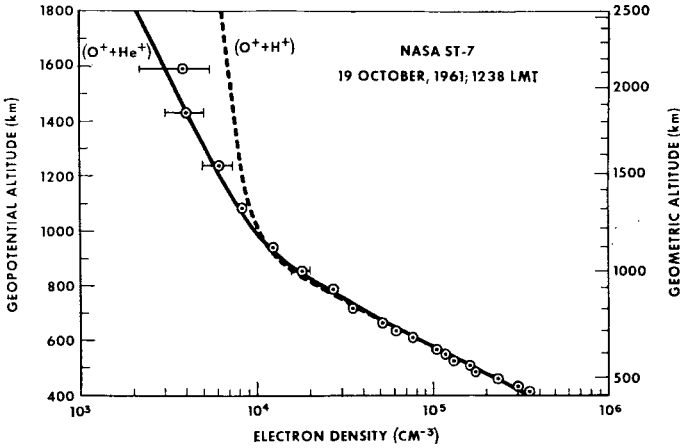


Fig. 12. Indirect detection of helium ions from electron density profile obtained on a Scout rocket.

700 km. The good agreement of the experimental n_+ values with the electron density obtained by rocket measurement and with the value of n_e measured by an ionosonde at the F2 peak speaks well for the validity of the data.

It can be shown from the theoretical curve provided by BAUER (curve A in Figure 5) that the experimental ion density profile corresponds most closely to a three-

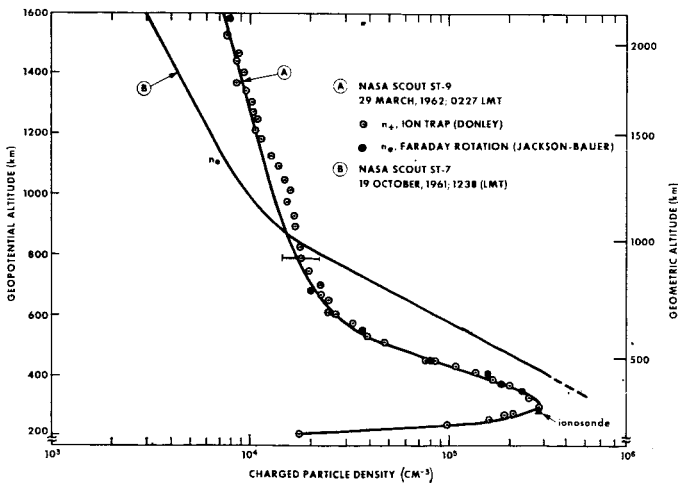


Fig. 13. Scout rocket measurements of the diurnal variation of the upper ionosphere.

constituent mixture rather than O^+ and H^+ . The closest fit of the experimental points to the theoretical curve in the ion transition altitude leads to an estimate of less than 300 km for the thickness of the helium ion layer. The discontinuity in the experimental n_+ values at geopotential altitudes between 900 and 1100 km probably can be explained from the observation that the spacecraft went from a dark to a sunlit condition

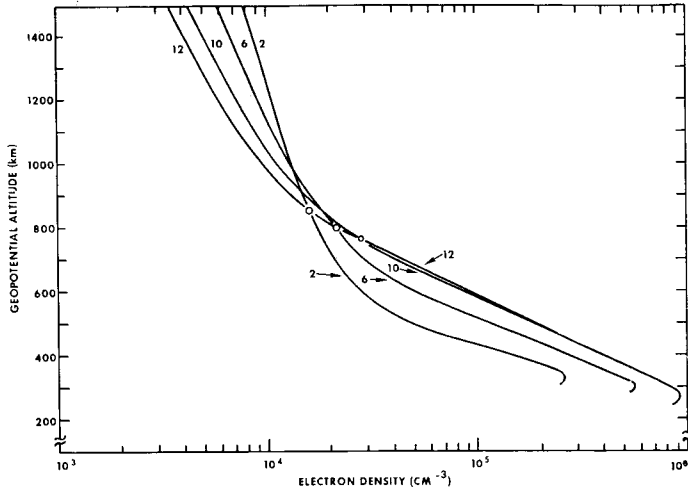


Fig. 14. Qualitative model of the detailed diurnal variation of the upper ionosphere.

in this region. The discontinuity probably represents a transient departure from temperature equilibrium.

Curve B in Figure 13 is the electron density profile replotted from Figure 12 to illustrate an observed diurnal variation of charged particle density in the upper ionosphere. The observation that the nighttime electron densities actually exceed those for daytime conditions at geometric altitudes greater than 1000 km should not be surprising since the lower ion transition altitude and the large scale height for protons overcompensate for the higher daytime atmospheric temperature and the higher daytime electron density at the F2 peak.

SAYERS, ROTHWELL and WAGER (1962) claim to have discovered a new ionization ledge with peak densities located at geometric altitudes varying from 1200 km at midnight down to 600 km at midday. The apparent negative scale heights gradients which were reported carry an implication of an ionization source in this altitude region. Discontinuities in charged particle density profiles perhaps can be expected at sunrise and at the equatorial anomaly, yet the discovery of this ledge is claimed throughout the day and for all latitudes traversed by the Ariel satellite. SAYERS *et al.* constructed their profiles from rf probe measurements of electron density at the satellite position. The nature of the Ariel orbit during the time the data were obtained was such that the altitude profiles are not time independent but rather represent observations taken over a change of several hours in local mean time. An alternative explanation, then, is that

these ledges are only apparent in that they do not represent altitude discontinuities but rather changes in ionization brought about by the difference in local time at various points in the Ariel orbit. This alternative explanation is illustrated qualitatively in Figure 14. The experimental curves in Figure 13 already illustrate the diurnal variation of the electron density in the upper ionosphere. The four curves shown in Figure 14 are inferred profiles for the hours indicated. They were constructed from a typical variation of the electron density at the F2 peak as observed for May (the month of the Ariel observations) by ionosondes, an atmospheric temperature variation taken from reference atmospheres, and the ion transition model of BAUER illustrated in Figure 11. It can be shown for a satellite which requires several hours of local time to traverse the 400–1200 km altitude region, that an apparent ionization ledge would be observed when the satellite passes through the higher altitude region at night and conversely when it passes through the lower altitude region during midday. Parenthetically, an interesting feature to note from Figure 14 is the approximate constancy with diurnal time of the electron density at a geopotential altitude of about 800 km (approximately 1000 km geometric).

9. The Altitude Dependence of Charged Particle Temperature

It is of considerable importance to compare electron (T_e), ion (T_i) and neutral gas (T_g) temperatures as a function of altitude because their interdependence perhaps is the most sensitive index of complex reactions, the understanding of which is the ultimate goal of upper atmosphere physicists. For the time being, it will be assumed that T_i and T_g are equal.

Because direct and indirect measurements of charged particle temperatures have been made under radically different conditions and because of the limitations of the kinetic gas temperature models, various investigators have provided conflicting answers to the important question of temperature equilibrium between electrons and heavy constituents under daytime conditions. It generally is accepted that temperature equilibrium predominates at all altitudes during the night under quiet solar conditions. In this section it will be shown for a restricted set of latitude and atmospheric conditions that during midday temperature equilibrium exists below 150 and above 450 km, in accordance with recent reviews (BAUER and BOURDEAU, 1962; BOURDEAU and BAUER, 1962). It will be shown, on the other hand, that there is a substantial difference between spaceflight results and those from some ground-based radar incoherent backscatter experiments.

Before proceeding, it is important to define the term "temperature equilibrium". Actually because in the ionization process the electrons are created with high initial energies, their temperature will always be somewhat higher and only can approach T_g asymptotically in time depending on the efficiency of the energy transfer mechanism. Temperature equilibrium in this paper is defined as a difference between T_e and T_g which is smaller than the uncertainties in reference atmospheres and in spaceflight experimental methods of measuring charged particle temperatures. It is estimated,

perhaps optimistically, that these uncertainties together are about ten percent of the absolute value of T_g .

Our knowledge of the behavior of the neutral gas temperature is based principally on atmospheric densities computed from satellite drag observations and an assumed atmospheric composition. Values of T_g so derived must be considered approximate

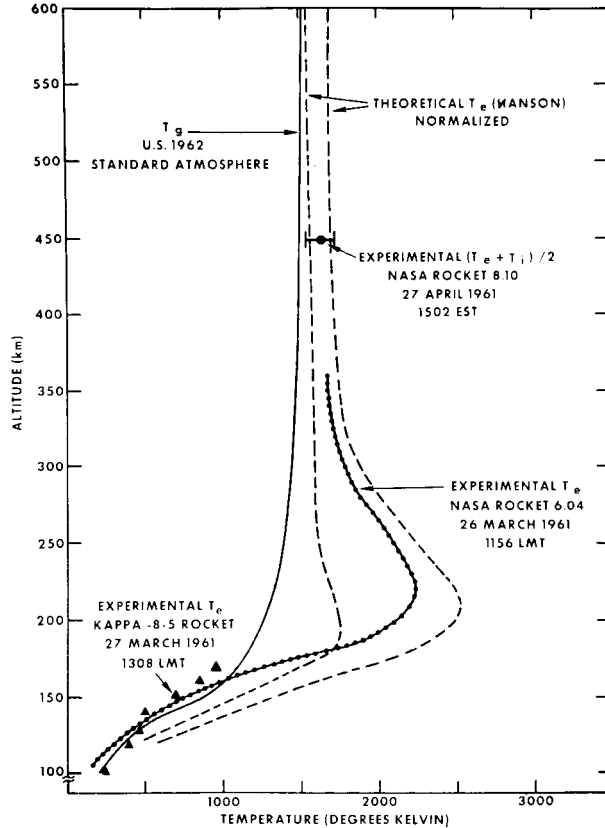


Fig. 15. Comparison of the altitude dependence of neutral gas and experimental and theoretical electron temperatures at mid-latitudes under quiet solar conditions.

principally because of the observational gap in atmospheric composition. Plotted as a solid line in Figure 15 is the altitude dependence of the neutral gas temperature published by the U.S. Committee on Extension to the Standard Atmosphere (SISSEWINE, 1962). The COESA reference atmosphere was selected because it depicts "typical mid-latitude year-round conditions averaged for daylight hours and for the range of solar activity that occurs between sunspot minimum and sunspot maximum", conditions which most closely approximate those under which the charged particle temperature measurements have been made.

The earliest theoretical study of the temperature difference between T_e and T_g was

advanced by HANSON and JOHNSON (1961). Because of improved cross-sectional and solar radiation data and because of the omission of an important process (electron impact excitation of vibrational levels of molecular nitrogen), this work now must be considered superseded by more recent theoretical models (HANSON, 1962b; DALGARNO, MCELROY and MOFFETT, 1962). These models, which consider ionization by solar radiation only, involve several expansions (depending upon the energy transfer mechanisms) of the equation:

$$(T_e - T_g)/\tau = \frac{2q'E}{3n_e k} \quad (11)$$

where q' is the rate at which photoelectrons of energy E are released and τ is the time which it takes for these electrons to transfer their excess energy in various processes. Considerations are given to loss of this excess energy by (a) inelastic ionizing collisions with neutral particles, (b) inelastic exciting collisions with neutral particles where the energy is stored either in metastable or vibrational states, (c) energy transfer to ambient ions and (d) elastic collisions with ambient electrons. In all but the latter case, much of the excess energy of the newly-created photoelectrons is removed before they selectively heat the ambient electron gas.

HANSON (1962b) computed four models for the case where the daytime temperature in the isothermal region is 1200° K. These four models are based on two different altitude-dependent values for the electron production rate and two different assumptions for the excess photoelectron energy. The two extremes of these four curves are plotted in Figure 15. It is seen that the maximum predicted departure from temperature equilibrium proposed by HANSON corresponds closely to the altitude of maximum electron production illustrated in Figure 8. Possible small errors have been introduced in Figure 15 by assuming that the value of $T_e - T_g$ actually computed by HANSON are invariant when T_g in the isothermal region is raised from 1200° K as used in his reference atmosphere and the 1500° K value used here.

At present, an experimental determination of the complete altitude dependence of $T_e - T_g$ can be accomplished only empirically by comparing Langmuir probe measurements of electron temperature obtained on vertical sounding rockets with a reference atmosphere. Langmuir probes have required considerable development in order to overcome problems associated with the disturbance introduced into the medium by a conducting body. Extremely high electron temperatures were reported from observations of large potentials on the Sputnik III spacecraft (KRASSOVSKY, 1959). However, it is dangerous to infer electron temperatures by this indirect method because of the probability of a vehicle potential which is artificially controlled by differing surface work functions, for example, than by ambient ionospheric parameters.

It wasn't until 1961 that electron temperatures close to accepted kinetic gas values were first reported for the E region by Japanese investigators (AONO *et al.*, 1961) and for the upper ionosphere by use of the Explorer VIII Satellite (SERBU, BOURDEAU and DONLEY, 1961). However, these data by themselves do not provide a complete altitude profile of T_e . The Japanese data, which represent an average from two separate

devices flown simultaneously, were obtained over the altitude interval between 100 and 170 km and are plotted in Figure 15. A separate rocket (NASA 6.04) containing an ejectable symmetric bipolar probe was launched at approximately the same latitude and time. These results (BRACE, 1962) are plotted as the dotted curve in Figure 15. Parenthetically, they represent a significant modification by BRACE of the data which was first reported in a preliminary form (SPENCER, BRACE and CARIGNAN, 1962). The error spread of the overall curve has been estimated by BRACE to be ± 10 percent. Also plotted in Figure 15 is the atmospheric temperature computed on the assumption of temperature equilibrium by JACKSON and BAUER (1961) from their experimental electron density profile. This value, applicable to the region above 450 km, was selected because it was taken under identical solar conditions (indexed by observed solar decimeter flux observations) as the two electron temperature profiles. Considering the uncertainty in the reference atmosphere and the experimental error flag, it can be concluded *for these particular solar conditions* that temperature equilibrium exists below 150 km and above 450 km. Also there is reasonable agreement between the experimental results and the theoretical work of HANSON.

DALGARNO *et al.* (1962) have proposed four theoretical electron temperature models for a given noontime value of T_g . The end result in the form of the altitude dependence of $T_e - T_g$ for $T_g = 2000^\circ$ K is presented in Figure 16. The alternative curves are based on some reduction of excess photoelectron energy by (a) ionizing collisions alone, (b) including possible energy transfer through exciting collisions leading to the metastable state, (c) excluding (b) but including possible energy transfer through exciting collisions leading to the vibrational state and (d) a combination of all energy transfer mechanisms. Also plotted in Figure 16 are experimental values for $T_e - T_g$ taken from Figure 15. It is tempting from the agreement of the experimental data with curves a and b in Figure 16 to suggest that excess photoelectron energy in the lower altitude regions is removed principally by a combination of ionizing collisions and exciting collisions leading to the metastable state.

HANSON (1962b) has advanced a theoretical possibility based on low thermal contact between the ions and neutral particles that the ion temperature at very high altitudes could depart from the neutral gas temperature and approach the electron temperature. He estimates that such a transition could possibly occur in the 600–1000 km region. It is extremely difficult to corroborate this possibility from experimental observations because the differences between T_e , T_i and T_g are small at these altitudes. The daytime electron density profile illustrated in Figure 12 shows that the sum of the electron and ion temperatures taken in both the He^+ and O^+ regions are approximately the same. The constancy of this sum with altitude also can be inferred in published data (KING, 1963) from the Alouette Topside Sounder Satellite. This is evidence either that the differences in the electron, ion and neutral gas temperatures are vanishingly small above 450 km or that the ion temperature transition proposed by HANSON occurs above 1000 km, if at all.

The agreement of Langmuir probe results with the theoretical work of HANSON and DALGARNO *et al.* suggests that, at midday, temperature equilibrium exists

below 150 km and above 450 km whenever ionization is the result of solar radiation alone. However, because of the small number of observations, generalization of this conclusion may be premature. SPENCER, BRACE and CARIGNAN (1962) have made rocket flights at auroral latitudes and into a disturbed mid-latitude ionosphere. For these conditions they report E and F2 region electron temperatures which are systematically higher than the quiet mid-latitude results. The difference is perhaps re-

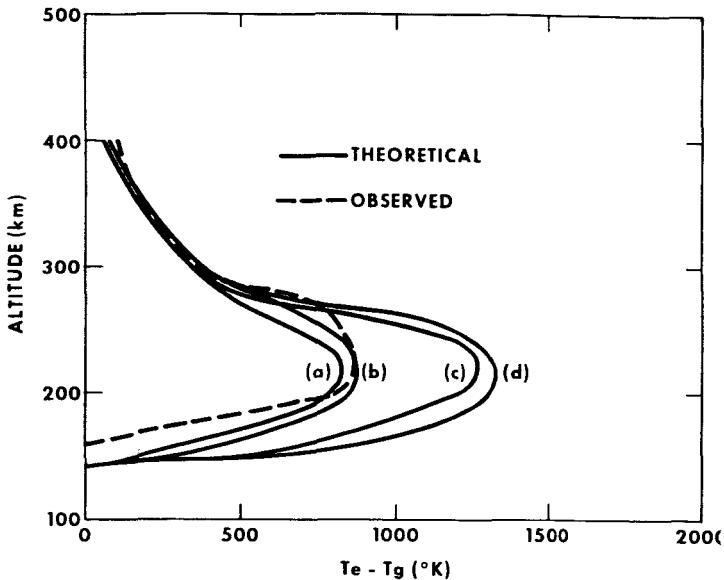


Fig. 16. Theoretical (DALGARNO, 1962) and experimental (BRACE, 1962) models of the altitude dependence of the difference between electron and neutral gas temperatures at mid-latitudes under quiet solar conditions.

presentative of the influence of corpuscular radiation. There is also a small possibility that the electron temperatures reported for disturbed conditions by SPENCER *et al.* (1962) are not representative of the most abundant electrons. Their symmetric Langmuir probe samples only those electrons which can overcome a retarding potential of a few tenths of a volt. Since a Maxwellian electron energy distribution has been established for quiet solar conditions, the data reported by BRACE and plotted in Figure 15 and 16 should be representative of the entire electron population. However, the existence of a Maxwellian energy distribution under disturbed ionospheric conditions has not been verified.

The spaceflight observations in a quiet daytime ionosphere are consistent with the conclusions (BOWLES, OCHS and GREEN, 1962) from ground-based radar incoherent backscatter experiments that the electron and ion temperatures are in equilibrium in the upper ionosphere except at sunrise and during disturbed conditions. EVANS (1962), on the other hand, also using backscatter experiments reports different results. The principal differences for which no explanation can be given here are: (a) EVANS reports temperature equilibrium at 200 km, an altitude at which both theory and the

spaceflight observations show a significant departure from equilibrium; (b) the ratio T_e/T_i is 1.6 and constant above 300 km as reported by EVANS whereas both theory and the spaceflight observations show this ratio decreasing with altitude above 250 km; (c) EVANS reports that the sum of T_e and T_i increases with altitude up to 700 km whereas it is concluded from many rocket measurements of charged particle density profiles that this sum is constant with altitude in the upper ionosphere. The results obtained by EVANS also are inconsistent with the diurnal variation of charged particle temperatures at altitudes above 450 km, which is discussed in the succeeding section.

10. Diurnal Variation of Upper Ionosphere Temperatures

In this section, a comparison will be made of the diurnal variations of charged particle and neutral gas temperatures for the isothermal altitude region above 450 km. At these altitudes our knowledge of T_g generally is derived from satellite drag observations and an assumed atmospheric composition. The drag observations show that density variations are correlated with solar activity. Although not the source of upper atmosphere heating, solar decimeter radiation which is observable at the earth's surface is an indicator of this interrelationship. For a given level of solar activity JACCHIA (1962), HARRIS and PRIESTER (1962) and PAETZOLD (1962) conclude:

- (1) The neutral gas temperature has its maximum value in mid-afternoon;
- (2) This maximum would occur at sunset if absorption of solar ultraviolet radiation was the only source of atmosphere heating;
- (3) Consequently, there is a second source of heating associated with the solar wind;
- (4) These conclusions apply to the atmosphere at low latitudes.

In the preceding section it was shown for a specific set of observations taken at mid-latitudes that the electron and neutral gas temperatures have approximately the same value above 450 km, which is consistent with theoretical computations based on solar ultraviolet radiation as the sole ionizing source. If the low latitude ionization generally can be explained entirely by solar ultraviolet radiation and if, as claimed, the diurnal variation characteristic of the neutral atmosphere requires a second heat source, then the additional heating mechanism should be one which is least likely to selectively heat either the light or heavy atmospheric constituents. The heating by hydromagnetic waves proposed by DESSLER (1959) probably meets these criteria. It is not possible from the charged particle temperature data presented in this section to infer a diurnal neutral gas temperature variation precisely enough to confirm or deny the hypothesis of a second heat source which is effective at mid-latitudes.

There is some variance in reference atmospheres in the absolute magnitude of the temperature at diurnal maximum and minimum. The model attributed to PRIESTER by JASTROW (1961) which is plotted in Figure 17 has an average daytime value consistent with the COESA standard atmosphere. It corresponds to a level of solar activity for which the observed solar decimeter (10.7 cm) radiation flux is $150 \text{ w/m}^2/\text{cps}$. Other models (HARRIS and PRIESTER, 1962; JACCHIA, 1962) generally show somewhat lower

temperatures at diurnal maximum. Also plotted in Figure 17 are experimental values all taken at mid-latitudes of (a) the neutral gas temperature measured directly by BLAMONT (1961, 1962) using rockets containing sodium vapor release experiments, (b) direct measurements of electron temperature from the Explorer VIII Langmuir probe (SERBU *et al.*, 1961) and (c) values of T_g computed from rocket measurements of electron scale height on the assumption of temperature equilibrium, for which $T_g = \frac{1}{2} (T_e + T_i)$. These data were obtained at various times and consequently have

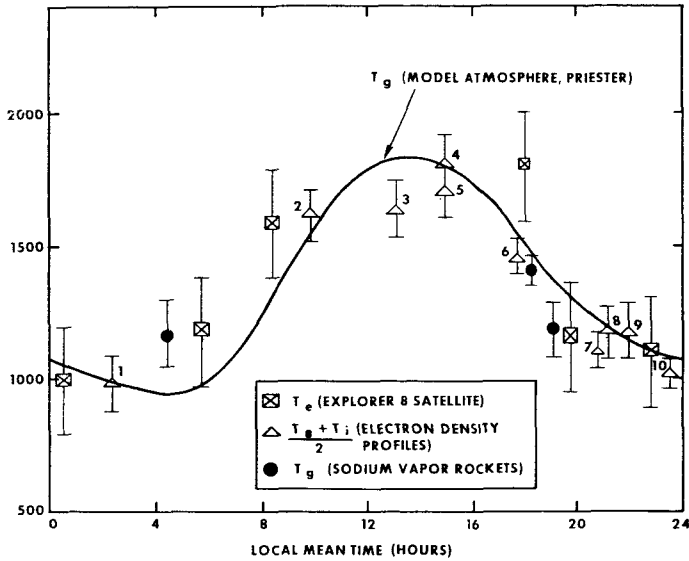


Fig. 17. Diurnal variation of upper atmosphere temperature for altitudes above 450 km at mid-latitudes, solar decimeter flux = 150×10^{-22} w/m²/cps.

been normalized by this author to the same solar activity (10.7 cm flux = 150 w/m²/cps) using the empirical relation given by HARRIS and PRIESTER (1962). The temperatures derived from electron or ion profiles are taken (1) from DONLEY (1963), (2), (8) and (9) from BERNING (private communication), (3) from BAUER and JACKSON (1962), (4) from JACKSON and BAUER (1961), (5) from HANSON (1962), (6) and (10) from KNECHT and RUSSELL (1962), and (7) from HANSON and MCKIBBIN (1961).

It is tempting from the general agreement of the neutral gas temperatures with the Explorer VIII electron temperatures and with the values of $\frac{1}{2}(T_e + T_i)$ derived from charged particle density profiles, all illustrated in Figure 17, to infer support for the conclusion reached in the previous section that temperature equilibrium exists above 450 km for most of the day under quiet ionospheric conditions at mid-latitudes. However, the empirical method of comparison used in Figure 17 can only be an approximate test of equilibrium, because except for BLAMONT's data, the neutral gas temperature is an inferred parameter and because the preciseness of normalizing data taken at different times to the same level of solar activity has not been established.

The Explorer VIII electron temperature device is a gridded trap which experimentally eliminates unwanted photocurrent effects. The error flags shown in Figure 17 result from a limited volt-ampere curve resolution imposed by the telemetry system. There possibly is an additional small error associated with the electrical transparency characteristics of the grids used to remove the photocurrent effect (SERBU *et al.*, 1961). The absence of an on-board tape recorder prevented detailed analyses of the diurnal electron temperature variation and the detection of latitude effects.

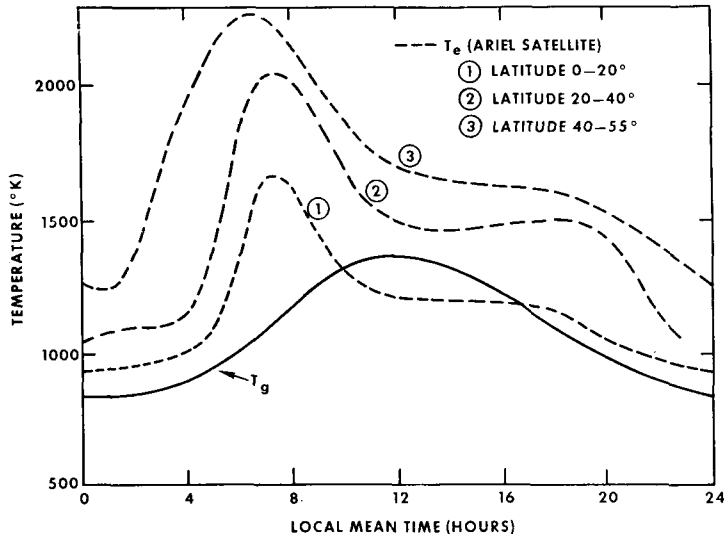


Fig. 18. Possible latitude dependence of the diurnal variation of electron temperature for altitudes above 450 km, solar decimeter flux = 100×10^{-22} w/m²/cps.

A different type of Langmuir probe now has been flown on the Ariel satellite. Basically an asymmetric probe with the sensor located on a boom away from the main spacecraft, the experiment tends to suppress such unwanted effects as varying vehicle potentials and photocurrent and magnetic field modulation of the electron current by measuring the electron temperature in an extremely short time interval. The availability of an on-board tape recorder has permitted the investigators to report the most detailed diurnal electron temperature variation yet obtained and additionally to separate the data according to latitude. Their preliminary results as reported (WILLMORE, BOYD and BOWEN, 1962) are shown in Figure 18. The three curves, each representing a different latitude region were obtained at a time when the 10.7 cm solar radiation flux averaged 100 w/m²/cps. The PRIESTER model of the diurnal variation of the neutral gas temperature in Figure 17 has been normalized to this lower level of solar activity and replotted in Figure 18 for comparison.

The Ariel data were analyzed on the assumptions that the temperature above 450 km is isothermal and that there is a symmetrical distribution about the equator. WILLMORE *et al.* point out that the salient features are a general rise in temperature

and a less pronounced diurnal variation at high latitudes and that both of these observations are consistent with significant atmospheric heating by particles being dumped at high latitudes.

Another salient feature of the Ariel data is the high electron temperature observed in the sunrise period. This is not inconsistent with the experimental results in Figure 17 because of the observational gap in the latter data during this period. The sunrise effect in the Ariel data is evidence for a departure from temperature equilibrium. The diurnal shapes of the curves suggest that temperature equilibrium is re-established toward midday. The observation of a departure from temperature equilibrium at sunrise is consistent with the conclusions from one set of ground-based backscatter results (BOWLES, 1962) but not with EVANS (1962) who reports maximum departure from equilibrium at noon. A higher ratio T_e/T_i at sunrise than at noon is more consistent with what would be expected from a cursory extension to the theoretical observation (HANSON, 1962) that T_e/T_i is directly proportional to q/n_e^2 above the F2 peak. The electron production rate, q , is in turn proportional to atmospheric density. It can be shown from a comparison of the atmospheric density variation derived from satellite drag with the electron density profiles illustrated in Figure 14 that the ratio q/n_e^2 and thus that T_e/T_i should be higher at dawn than at noon.

It would be premature to draw firm conclusions regarding additional ionizing and heating sources from the diurnal comparisons of upper ionosphere electron and neutral gas temperatures shown in Figures 17 and 18. The experimental charged particle observations in Figure 17, for example, were obtained over a period of more than one year. The accuracy of the process of normalizing these data to the same level of solar activity quite likely introduces enough error that the diurnal shape of the indirectly-derived neutral gas temperature cannot be confirmed. Consequently, the hypothesis of a second heat source at low latitudes also cannot be confirmed.

The midday values of T_g proposed by PRIESTER and which is applicable to low latitudes fall in between the two lower latitude electron temperature curves measured on the Ariel satellite. No conclusion can be drawn from the different diurnal shapes of T_e and T_g in Figure 18, principally because two refinements in the analysis of the Ariel data are required. Firstly, there is no evidence that the Ariel results have been normalized for the day-to-day fluctuations in solar activity which can amount to a ten percent correction. This normalization could alter both the diurnal shape of the individual electron temperature curves and the amplitude of the latitude effect. Secondly, it would be expected again from a cursory theoretical analysis that the electron temperature in the upper ionosphere during the sunrise period would be altitude dependent. Since the present analysis of the Ariel data assumes no altitude effect, this also could alter the diurnal shape of the individual electron temperature curves. With reference to the diurnal variation of T_g , the Ariel data suggest a latitude effect which up until now has not been seriously considered in neutral gas models. This latitude effect in turn suggests that other heat and ionization sources in addition to direct solar radiation need to be considered in a description of even the normal auroral ionosphere.

11. Summary

Spaceflight observations made in recent years are most consistent with the following general conclusions:

(1) The principal ionizing agents for the D region under quiet solar conditions at an epoch corresponding to the middle of the solar cycle are cosmic radiation for the region below 70 km and Lyman α radiation at altitudes between 70 and 85 km. The negative ion abundance at all D region altitudes has been underestimated theoretically.

(2) X-radiation (2–8 A) and energetic protons, which are respectively responsible for Sudden Ionospheric Disturbances and Polar Cap Absorption Events, lead to a D region electron density enhancement of about two orders of magnitude.

(3) The principal ions produced in the lower ionosphere are N_2^+ , O_2^+ and O^+ . The ions which exist in greatest abundance are NO^+ , O_2^+ and O^+ . These ionization characteristics result from the combined influence of solar ultraviolet and X-radiation in the E region with ultraviolet radiation becoming the dominant source in the F region.

(4) The average E region electron density decreases by about two orders of magnitude at night. Some types of sporadic-E ionization have a depth of less than one kilometer and a horizontal dimension greater than 70 km. Other types have a smaller horizontal dimensions. There is a first order increase of the electron density in a sporadic E-layer.

(5) The formation of the F2 peak is best explained by the combined altitude dependence of the electron production rate, electron loss by an attachment like process and diffusion.

(6) The constant electron-ion scale height which is observed for altitude intervals of a few hundred kilometers above the F2 peak is evidence that the upper ionosphere is isothermal and in diffusive equilibrium.

(7) The upper ionosphere is characterized by the presence of three ionic constituents (O^+ , He^+ , H^+) each predominating in a different altitude region. The thickness of the helium ion layer has a large diurnal variability. The control which these ionic constituents exercise over the electron density distribution is such that the electron density is generally higher at midday below 1000 km, shows a small diurnal variation near 1000 km, and is generally higher at altitudes between 1000 and 2000 km at night.

(8) In an undisturbed mid-latitude ionosphere, it is generally accepted that temperature equilibrium can be expected at night. Significant departures from equilibrium can be expected at sunrise and during disturbed conditions. Toward midday under quiet mid-latitude conditions significant departures from equilibrium would be expected in the lower F region, but small differences between T_e , T_i and T_g are observed below 150 and above 450 km.

(9) Except for the sunrise anomaly the diurnal maximum and minimum values of electron temperature at mid-latitudes approximate the diurnal extremes of the neutral gas temperature in the upper ionosphere. An observed latitude dependence of electron

temperature suggest that corpuscular radiation is an important heat source at high latitudes.

12. Acknowledgements

I wish to acknowledge the helpful discussions with A. C. AIKIN, S. J. BAUER, L. H. BRACE, S. CHANDRA, L. G. SMITH and E. C. WHIPPLE. I also wish to thank L. H. BRACE, J. L. DONLEY, J. E. JACKSON, S. J. BAUER, E. SCHAEFFER and especially the investigators associated with the Ariel satellite for making their results available in advance of publication,

References

- AIKIN, A. C.: 1962a, *International Symposium on Equatorial Aeronomy*, Lima, Peru, September 25.
 AIKIN, A. C.: 1962b, *Goddard Space Flight Center Report X-215-62-132*.
 AONO, Y., HIRAO, K. and MIYAZAKI, S.: 1961, *Journ. Rad. Res. Lab.*, Japan **8**, 453.
 BATES, D. R.: 1956, in: *Solar Eclipses and the Ionosphere*, Beynon and Brown, editors, Pergamon Press, p. 184.
 BATES, D. R. and PATTERSON, T. N. L.: 1961, *Plan. Space Sci.* **5**, 257.
 BAUER, S. J. and JACKSON, J. E.: 1962, *Journ. Geophys. Res.* **67**, 1675.
 BAUER, S. J.: 1962, *Journ. Atmos. Sci.* **19**, 276.
 BAUER, S. J.: 1963, *Nature* January.
 BAUER, S. J. and BOURDEAU, R. E.: 1962, *Journ. Atmos. Sci.* **19**, 218.
 BELROSE, J. S. and BURKE, M. J.: 1961, *URSI meeting*, Washington, D.C., May 4.
 BERNING, W. W.: 1960, *Journ. Geophys. Res.* **65**, 2589.
 BLAMONT, J., 1961, in: *Space Research II* (ed. by H. C. VAN DE HULST *et al.*), North-Holland Publ. Comp.; p. 974.
 BOURDEAU, R. E., WHIPPLE, E. C., and CLARK, J. F.: 1959, *Journ. Geophys. Res.* **64**, 1363.
 BOURDEAU, R. E.: 1961, in: *Space Research II* (ed. by H. C. VAN DE HULST *et al.*) North-Holland Publ. Comp., p. 554.
 BOURDEAU, R. E., DONLEY, J. L., SERBU, G. P., and WHIPPLE, E. C. 1961, *Journ. Astronaut. Sci.* **8**, 65.
 BOURDEAU, R. E. and BAUER, S. J.: 1962, *Third Intern. Space Sciences Symposium*, Washington, D.C., May.
 BOURDEAU, R. E., DONLEY, J. L., WHIPPLE, E. C. and BAUER, S. J.: 1962, *Journ. Geophys. Res.* **67**, 467.
 BOWLES, K. L., OCHS, G. R., and GREEN, J. L.: 1962, *Journ. Research, National Bureau of Standards* **66**, 395.
 BRACE, L. H.: 1962, *University of Michigan Scientific Report*. JS 3, 03599-11-F.
 CHANDRA, S.: 1963, *Journ. Geophys. Res.* **68**.
 CHUBB, T. A., FRIEDMAN, H., and KREPLIN, R. W.: 1960, *Journ. Geophys. Res.* **65**, 1831.
 DALGARNO, A., MCELROY, M. B., and MOFFETT, R. J.: 1962, *Geophys. Corp. of America, Tech. Report* 62-11-N.
 DESSLER, A. J.: 1959, *Journ. Geophys. Res.* **64**, 397.
 DONAHUE, T. M.: 1962, *Space Sci. Rev.* **1**, 135.
 DONLEY J. L.: 1963, *Journ. Geophys. Res.* **68**.
 DUNGEY, J. W.: 1955, *The Physics of the Ionosphere*, London, Physical Society, p. 229.
 EVANS, J. V.: 1962, *Journ. Geophys. Res.* **67**, 4914.
 FAIRE, A. C. and CHAMPION, K. S.: 1959, *Phys. Rev.* **113**, 1.
 FRIEDMAN, H.: 1959, *Proc. Inst. Radio Engrs* **47**, 272.
 FRIEDMAN, H.: 1962, *Astronautics* **14**, August.
 GARDNER, F. F. and PAWSEY, J. L.: 1953, *Journ. Atmos. and Terr. Phys.* **3**, 231.
 HALE, L. C.: 1961, *Journ. Geophys. Res.* **66**, 1554.
 HANSON, W. B. and JOHNSON, F. S.: 1961, *Les Congrès et Colloques de L'Université de Liège* **20**, 390.
 HANSON, W. B. and MCKIBBIN, D. D.: 1961, *Journ. Geophys. Res.* **66**, 1667.
 HANSON, W. B.: 1962a, *Journ. Geophys. Res.* **67**, 183.
 HANSON, W. B.: 1962b, *Third Intern. Space Sciences Symp.*, Washington, D.C., May.
 HARRIS, I. and PRIESTER, W.: 1962, *Journ. Geophys. Res.* **67**, 4585.

- HINTEREGGER, H. E., DAMON, K. R., and HALL, L. H.: 1959, *Journ. Geophys. Res.* **64**, 961.
- HINTEREGGER, H. E. and WATANABE, K.: 1962, *Journ. Geophys. Res.* **67**, 3373.
- HULBURT, E. C.: 1938, *Phys. Rev.* **53**, 344.
- ICHIMUJA, T., TAKAYAMA, K., and AONO, Y.: 1959, *Journ. Radio Res. Lab.*, Japan **13**, 155.
- ISTOMIN, V. G.: 1960, *Artificial Earth Satellites 2*.
- JACCHIA, L.: 1962, *Third Intern. Space Sciences Symp.*, Washington, D.C., May.
- JACKSON, J. E. and KANE, J. A.: 1959, *Journ. Geophys. Res.* **64**, 1074.
- JACKSON, J. E. and BAUER, S. J.: 1961, *Journ. Geophys. Res.* **66**, 3055.
- JASTROW, R.: 1961, *25th Wright Brothers Lecture*, Washington, D.C., December.
- JOHNSON, C. Y., MEADOWS, E. B. and HOLMES, J. C.: 1958, *Journ. Geophys. Res.* **63**, 443.
- KANE, J. A.: 1959, *Journ. Geophys. Res.* **64**, 133.
- KANE, J. A.: 1960, *AGARD meeting*, Athens, Greece, March.
- KASNER, W. H., ROGERS, W. A., and BIONDI, M. A.: 1961, *Phys. Rev. Letters* **7**, 321.
- KING, J., 1963, *Nature*, in press.
- KNECHT, R. W. and RUSSELL, S.: 1962, *Journ. Geophys. Res.* **67**, 1178.
- KRASNUSKIN, P. E. and KOLESNIKOV, N. L.: 1962, *Dokl. Akad. Nauk. SSSR* **146**, 596.
- KRASOVSKY, V. I.: 1959, *Proc. Inst. Radio Engrs. N. Y.* **41**, 289.
- KREPLIN, R. W., CHUBB, T. A., and FRIEDMAN, H.: 1962, *Journ. Geophys. Res.* **67**, 2231.
- LINDSAY, J. L.: 1962, *Third International Symposium on Space Phenomena*, Detroit, Michigan, October.
- LOEB, L. B.: 1955, *Basic Processes of Gaseous Electronics*, University of California Press, p. 42.
- MAEHLUM, B. and O'BRIEN, B. J.: 1962, *Journ. Geophys. Res.* **67**, 3281.
- MANGE, P.: 1961, *Journ. Geophys. Res.* **66**, 2263.
- MOLER, W. F.: 1960, *Journ. Geophys. Res.* **65**, 1459.
- NICOLET, M.: 1945, *Mem. Inst. Roy. Meteorol., Belgium* **19**, 124.
- NICOLET, M. and AIKIN, A. C.: 1960, *Journ. Geophys. Res.* **65**, 1469.
- NICOLET, M.: 1961, *Journ. Geophys. Res.* **66**, 2263.
- NICOLET, M. and KOCKARTS, G.: 1962, *Third Intern. Space Sciences Symposium*, Washington, D.C., May.
- PAETZOLD, H. K.: 1962, *Journ. Geophys. Res.* **67**, 2741.
- POUNDS, K. A. and WILLMORE, A. P.: 1962, *International Conference on the Ionosphere*, London, July.
- POPPOFF, I. G. and WHITTEN, R. C.: 1962, *Journ. Geophys. Res.* **67**, 2986.
- RATCLIFFE, J. A., SCHMERLING, E. R., and SETTY, C. S.: 1956, *Phil. Trans. Roy. Soc.* **248**, 621.
- RATCLIFFE, J. A. and WEEKES, K.: 1960, *Physics of the Upper Atmosphere*, RATCLIFFE, editor, Academic Press.
- SAYERS, J., ROTHWELL, P., and WAGER, J. H.: 1962, *Nature* **4847**, 1143.
- SAGALYN, R. C. and SMIDDY, M.: 1963, *Journ. Geophys. Res.* **68**, 199.
- SCHAEFFER, E. J.: 1963, *Journ. Geophys. Res.* **68**, 1175.
- SERBU, G. P., BOURDEAU, R. E., and DONLEY, J. L.: 1961, *Journ. Geophys. Res.* **66**, 4313.
- SEDDON, J. C. and JACKSON, J. E.: 1958, *Ann. de Geophys.* **14**, 456.
- SISSENIWIINE, N.: 1962, *Astronautics*, August, p. 52.
- SMITH, L. G.: 1961a, *AGU meeting*, Washington, D.C., April.
- SMITH, L. G.: 1961b, *AGU meeting*, Los Angeles, California, December 27.
- SPENCER, N. W., BRACE, L. H., and CARIGNAN, G. R.: 1962, *Journ. Geophys. Res.* **67**, 157.
- TAYLOR, H. A. and BRINTON, H. C.: 1961, *Journ. Geophys. Res.* **66**, 2587.
- ULWICK, J. C. and PEISTER, W.: 1962, *Third Intern. Space Science Symposium*, Washington, D.C., May.
- VAN ZANDT, T. E. and BOWLES, K. L.: 1960, *Journ. Geophys. Res.* **65**, 2627.
- VEGARD, L.: 1938, *Geophys. Publ.* **5**.
- WATANABE, K., MARMO, F. F., and PRESSMAN, J.: 1955, *Journ. Geophys. Res.* **60**.
- WATANABE, K. and HINTEREGGER, H. E.: 1962, *Journ. Geophys. Res.* **67**, 999.
- WHIPPLE, E. C.: 1959, *Proc. I.R.E.* **47**, 2023.
- WHIPPLE, E. C.: 1960, *Proc. Intern. Astronaut. Congress*, Stockholm, p. 99.
- WHITEHEAD, J. D.: 1960, *Nature* **188**, 567.
- WHITTEN, R. C. and POPPOFF, I. G.: 1961, *Journ. Geophys. Res.* **67**, 2986.
- WILLMORE, A. C., BOYD, R. L. F., and BOWEN, S. J.: 1962, *Conference on the Ionosphere*, London, July.
- WRIGHT, J. W.: 1960, *Journ. Geophys. Res.* **65**, 335.
- WULF, O. R. and DEMING, L. S.: 1938, *Terr. Magn. and Atmos. Elec.* **43**, 283.
- YONEZAWA, T. and TAKAHASHI: 1960, *Journ. Radio Research Lab.*, Japan **7**, 335.

ON THE INTERACTION BETWEEN A SPACECRAFT AND AN IONIZED MEDIUM

1. Introduction

Much of the data discussed in the preceding sections were obtained by direct measurements techniques (plasma probes). The success of experiments of this type is dependent upon an evaluation of the effects of the interaction between the spacecraft and the ionized atmosphere immediately surrounding it. An estimate of the errors which this interaction could introduce into the results can best be made by the respective investigators. However, it should be useful to readers unfamiliar with this class of experiments to present general considerations of this interaction and estimates of the relative confidence that can be placed on the electron and ion parameters obtained from plasma probes.

2. The Effects of RF Fields and of Contaminant Outgassing

Two factors artificially introduced by the spacecraft are the presence of radio-frequency fields due to telemetry transmissions and outgassing phenomena. The Japanese work (AONO *et al.*, 1962) on resonance probes demonstrates that if the frequency of rf transmissions exceeds the plasma frequency, there is a negligible perturbing effect. WHALE (1963) points out that this is so only for low values of radiated power. Low enough radiated rf power at a high enough frequency was maintained on the spacecraft from which data have been reported in the preceding sections of this paper to conclude that the rf field can be neglected.

The agreement of a direct satellite measurement of atmospheric density (SHARP, HANSON and MCKIBBIN, 1962) with that deduced indirectly from drag observations provides confidence that contaminants outgas soon enough to conclude a negligible effect from this factor on plasma probe results from orbiting vehicles. However, this effect must be taken into consideration for results obtained from vertical sounding rockets. ULWICK and PFISTER (1961), for example, find that outgassing contaminants actually mask the desired results for the case where care is not taken to seal the rocket's propellant tanks after engine burnout. Of the vertical sounding rocket data considered in this paper, that of BRACE (1962) presented in Figures 15 and 16 are expected to be most free of errors due to outgassing phenomena because of the care taken in separating the Langmuir probe from the rocket booster. The Japanese appear to have overcome the problem by placing their probes on booms extended a considerable distance from the rocket body. Of the rocket data discussed in this paper, those of SMITH (1961a, 1961b) shown in Figures 3 and 7 are most susceptible

to outgassing effects since he uses an active electrode flush-mounted on the rocket body. Even here, however, the good agreement which he obtains between ascent and descent data suggests a minimal error from the outgassing effect.

The remaining disturbance factors can be summarized as the sensitivity to spacecraft orientation of: (a) the potential of the spacecraft relative to the ambient medium- (b) the current (i_+) due to diffusion of positive ions from the medium to the spacecraft, (c) the current (i_e) due to diffusion of electrons from the medium to the spacecraft and (d) photocurrent (i_p) due to solar-radiation induced emission of electrons from the spacecraft surfaces. An experimental model of these interaction factors has been obtained from a set of experiments flown on the Explorer VIII satellite (BOURDEAU *et al.*, 1961). This model is qualitatively consistent with that proposed by GRINGAUZ and ZELIKMAN (1957). The Explorer VIII results are summarized herewith to permit subsequent general consideration of possible errors in the determination of ionospheric parameters by direct measurements techniques.

3. The Potential of a Spacecraft in the Ionosphere

The average equilibrium potential of a conducting body at rest where magnetic fields and solar radiation may be neglected is given by

$$\phi_0 = \frac{-kT_e}{e} \ln \frac{J_e}{J_+}, \quad (1)$$

where J_e and J_+ are the respective random electron and positive ion current densities which flow in the plasma in the absence of the conducting body. The respective current densities (J_e and J_+) are proportional to the charged particle density and the square root of the charged particle temperature and inversely proportional to the square root of the mass of the charged particles. Thus, for a condition near temperature equilibrium, the ratio J_e/J_+ is proportional to the square root of the ratio of the electron and ion masses. Because of the much smaller electron mass, $J_e \gg J_+$ and ϕ_0 will be negative for the stated conditions of a motionless body at night with no magnetic field.

For a moving body at night with no magnetic field, the average equilibrium potential is given by

$$\phi_0 = \frac{-kT_e}{e} \ln \frac{J_e S_e}{J_+ S_+}, \quad (2)$$

where S_e and S_+ are the areas over which the respective electron and ion currents are effective. Because of the higher electron mobility, $S_e > S_+$. Since J_e already is much greater than J_+ , ϕ_0 will be even more governed by the characteristics of the ambient electrons, specifically T_e . Indeed, the observation of a ϕ_0 of a few tenths of a volt negative for a nighttime condition on the Explorer VIII satellite is consistent with Equation 2 (using reasonable values of T_e) and thus lends confidence to a conclusion that the basic laws of kinetic theory are being obeyed for the case of an uncomplicated spacecraft.

For a daytime condition, the photocurrent effect which is of the same polarity as the current due to diffusion of positive ions from the medium to the spacecraft tends to drive the vehicle potential positive such that, for no magnetic field

$$\phi_0 = \frac{-kT_e}{e} \ln \frac{J_e S_e}{J_+ S_+ + J_p S_p}. \quad (3)$$

For a specific value of the ambient charged particle density, the diffusion and photocurrent effects can be expected to cancel with the convenient end result that ϕ_0 is zero. This was observed on the Explorer VIII satellite for the case where $N_e = 10^4 \text{ cm}^{-3}$, a value consistent with measured values of J_p and values of J_e computed from separate measurements of N_+ and T_e .

The preceding discussions of spacecraft potential were based on the simplifying assumption of no magnetic field. The motion of a spacecraft with velocity \mathbf{V} through a magnetic field \mathbf{B} will cause the vehicle surface to be non-equipotential. As a result, the vehicle potentials quoted above apply only to those measured on a plane passing through the center of the spacecraft and perpendicular to the vector representing the cross-product of the velocity and magnetic field vectors. The more general term for the potential of any surface element on a spacecraft is

$$\phi = \phi_0 + (\mathbf{V} \times \mathbf{B}) \cdot \mathbf{d}, \quad (4)$$

where \mathbf{d} is the vector distance from the surface element in question to the center of the spacecraft. A magnetic-field induced emf of 0.14 volts was measured across 30 cm on the Explorer VIII satellite (BOURDEAU *et al.*, 1961). This is consistent with a computation involving the insertion of known values of \mathbf{V} , \mathbf{B} and \mathbf{d} into Equation (4). More recently, WILLMORE *et al.* (1962) have reported a magnetic-field induced emf of 0.5 volts measured across a larger distance on the Ariel satellite.

The preceding discussion demonstrates that the behavior of the potential of a surface element on a spacecraft with a smooth configuration and without extensive protuberances is somewhat predictable. It can be expected that the potential of a surface element will undergo time changes which reflect different amounts of the overall vehicle area being exposed to various effects, particularly that due to the magnetic field. Thus as far as the effect of vehicle orientation modulation of spacecraft potential is concerned, it is necessary either to make a measurement during a time interval short compared to the orientation period or to resort to statistical averaging in extracting those geophysical parameters which are sensitive to the spacecraft potential.

4. The Reliability of Ion Parameter Measurements

In addition to the potential of the vehicle surface element at which the measurement is made, the other controlling factors in the determination of positive ion parameters is associated with velocity modulation of the ion current. Excepting the case of a measurement at the apogee of a vertical sounding rocket, the vehicle velocity greatly exceeds the thermal ion velocity. As a result, the current (i_+) flowing to a surface

element of area A pointed within 45° of the velocity vector is approximately given by

$$i_+ = e A N_+ V \cos \theta, \quad |\theta| < 45^\circ, \quad (5)$$

where θ is the angle between the surface element and the velocity vector. The larger vehicle velocity produces a "ram effect" such that i_+ would be expected to be a maximum when θ is zero and would vanish when the surface element is pointed into the wake of the vehicle. This was demonstrated on the Explorer VIII satellite by parametric scanning of i_+ as the vehicle spun. The effect illustrated in the top graph of Figure 19 was measured by a gridded device where, for this case, unwanted electron and photocurrents were experimentally removed. Equation (5) is valid whenever the potential of the surface element at which the measurement is being made is negative with respect to the plasma. It is seen from Equation (5) that the positive ion density (N_+) is computed from known parameters rather than resorting to assumptions about other ionic properties. Accordingly, reasonable assurance can be had that whenever the conditions of a negative surface element and a low value of θ are met, accurate values of N_+ will result. The validity of ion density determination whenever these two conditions are met has been demonstrated in several ways. Firstly, there is good agreement (DONLEY, 1963) between a direct measurement of n_+ and a separate but simultaneous radio-propagation method of measuring n_e . This agreement is illustrated in Figure 13. Secondly, consistent conclusions relative to the ionic composition (cf. Figure 11) and charged particle temperatures (cf. Figure 17) are reached whether one uses directly-measured ion density profiles or electron density profiles obtained by radio-propagation methods.

The history of the measurement of positive ion density by planar devices for the case of a negative surface element but where $90^\circ < \theta < 45^\circ$ or alternatively where the thermal ion velocity approaches or exceeds the spacecraft velocity is not as good. WHIPPLE (1959) has set forth the working equations for a planar ion trap which takes into account all values of the spacecraft-to-ion velocity ratio:

$$i_+ = eN_+A \left[V \cos \theta \left(\frac{1}{2} + \frac{1}{2} \operatorname{erf} x \right) + \frac{a_+ e^{-x^2}}{2\sqrt{\pi}} \right], \quad (6)$$

where a_+ is the ion thermal velocity and where

$$x = \frac{V \cos \theta}{a_+} - \frac{\phi_e}{kT_+}.$$

The above equations apply for the case where the ion sheath and the sensor used in making the measurement have the same geometry. There is experimental evidence that this assumption only holds approximately for the case of planar geometry. This was pointed out by BOURDEAU *et al.* (1961) from the observation that i_+ for $\theta = 90^\circ$ is too large as illustrated in the top graph of Figure 19. Thus, ion density values computed for such angles from the planar ion trap on the Explorer VIII satellite

would be too high. Similarly, BRACE (1962) finds that the n_+ values are ten percent too high at apogee of a sounding rocket although he gets good agreement with simultaneous measurements of electron density obtained by a radio-propagation experiment, at the lower altitudes where $V > a_+$.

Continuing the same reasoning, results show that Equation (6) cannot be applied exactly in determining other ionic parameters from planar sensors even when $\theta = 0$. For the condition of a ram ion current and a known vehicle velocity, it is possible

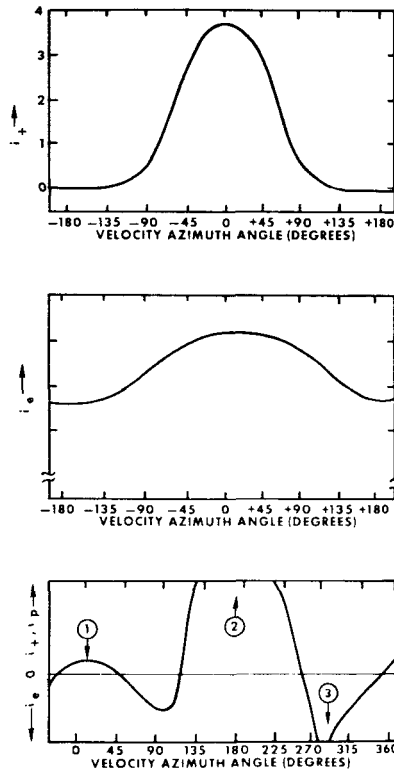


Fig. 19. Experimental observations of current exchange between the ionosphere and the Explorer VIII satellite.

to compute an idealized behavior for i_+ as a function of the potential of a surface element and as the ionic parameters of mass and temperature are varied. Such an idealized behavior for a constant T_+ with different values of m_+ is shown in Figure 10 where it is illustrated that a mixture of O^+ and He^+ is readily identifiable from one of O^+ and H^+ . It should be possible also to measure T_+ from the slope of the curves in the regimes where the current behavior is due to a single ionic constituent. However, Equation (6) was derived by WHIPPLE for the case of a planar sensor mounted on an infinite plane, a condition which only has been approximated on spacecraft flown to date. The exact conditions encountered are difficult to treat theoretically. It is most

likely because the geometry of the ion sheath is not planar that ion temperatures computed from planar ion traps by use of Equation (6) are generally too high. However, these considerations should not affect significantly the use of planar ion traps as ion composition measuring devices for the following reasons. The error in the measured ion temperature can be estimated from the difference between those experimentally-obtained by use of Equation (6) and estimates of the neutral gas temperature. It can be shown that within the limits of the error so obtained, the shapes of the curves illustrated in Figure 10 are not affected enough to alter the characteristic inflection point which identifies a mixture of O^+ and He^+ and the characteristic plateau which identifies a mixture of O^+ and H^+ . The method for demonstrating this involves maintaining a constant ionic mixture and varying the ionic temperature within the limits of the estimated error in T_+ in Equation (6). It should be emphasized that the preceding criticism of planar ion traps for T_+ determination does not apply to spherical ion traps such as those used on the Sputnik III and Ariel satellites. To the contrary, it would be expected that an equation for spherical geometry analogous to Equation (6) could be used with confidence for all ionic properties because of the high probability that the sensor and its surrounding ion sheath do have the same geometry. This conclusion is supported by the fact that experimental values of T_+ obtained by spherical devices are consistent with accepted values of the neutral gas temperature. These considerations in turn should permit the measurement of ion composition to a higher resolution than is possible with the planar ion traps.

To summarize the validity of ionic properties, it is expected that the ion density profiles obtained by HALE (1961), HANSON and MCKIBBIN (1961) and that reported by DONLEY (1963) in Figure 13 closely correspond to the true geophysical situations. This additionally is true of ion densities reported from Sputnik III. The ion composition results represented in Figures 10 and 11 also are expected to be approximately geophysically correct. Until additional theoretical work has been done on the ion sheath problem, ion densities obtained either when the ion thermal velocity approaches that of a spacecraft or from planar traps pointed at too large an angle from the velocity vector are expected to be incorrect. This is similarly true of the ion temperature parameter when obtained from a planar trap irrespective of the pointing angle. None of the data obtained for the latter two conditions has been used to derive geophysical conclusions in this paper. Parenthetically, the complicated behavior of the potential at a particular vehicle surface element has been taken into account in summarizing those data considered valid. It can be seen from Figure 10 that for negative potentials, the ion current is independent of the potential. Since for all cases used in the preceding sections the potential was negative when ion density was computed, the values of the latter parameter should not be subject to errors due to a changing vehicle potential, including the magnetic field induced emf effect. In ascertaining ion composition from the Explorer VIII planar ion trap, one is concerned with the behavior of i_+ as the potential is varied in a positive direction. Errors due to changes in overall vehicle potential were minimized, in this case, by obtaining a volt-ampere curve for changes

in orientation as little as 15 degrees (BOURDEAU *et al.*, 1961). The same philosophy of deriving ionic parameters in a short time interval was used by WILLMORE *et al.* (1962) for the obtainment of Ariel satellite ion composition and temperature results.

5. The Validity of Electron Parameter Measurement

The derivation of electron parameters from plasma probes is a degree more difficult than the case of positive ions principally because of the higher sensitivity to spacecraft potential effects. Digressing from this point a moment, the electron current to a particular surface element of constant potential will be dependent on the vehicle velocity, although to a lesser extent than the ions. This is because the thermal electron velocity exceeds even the satellite velocity. Electron current as a function of orientation relative to the velocity vector was uniquely measured on the Explorer VIII satellite (BOURDEAU *et al.*, 1961) by a device in which the positive ion and photocurrents were removed experimentally. These data are reproduced in the center graph of Figure 19. The amount of this modulation is consistent within a factor of two with what would be expected from an independent measurement of the electron temperature, the difference representing a gap in the theory of ion sheath behavior. This difference can be reflected in a measurement of electron density but should have a negligible effect on electron temperature determination.

Before proceeding to a fuller discussion of the validity of electron parameters, it is necessary to illustrate the behavior of the total net current flowing to and from a spacecraft surface element as the vehicle rotates. The net current includes the effects of ambient electron and positive ion diffusion and photoemission. Such data obtained from the use of an insulated portion of the Explorer VIII satellite by BOURDEAU *et al.* (1961) are reproduced in the bottom graph of Figure 19. Three major effects all of which mask velocity modulation of the electron current are to be noted. The first is the peak in the ram ion current as the sensor points in the direction of motion. The second and by far the major peak is due to photoemission as the sensor points toward the sun. The relative amplitude of this peak is dependent upon the ambient electron density which for this illustration was approximately 10^4 cm^{-3} . The third gross feature is the peak in the electron current which is due to the magnetic field effect. It occurs on the graph at a velocity azimuth angle between 270 and 360 degrees. At this position, the sensor was pointing in the $\mathbf{V} \times \mathbf{B}$ direction, the position of the most positive potential. For this reason, the peak in i_e shown in Figure 19 is to be expected.

All of the factors brought out by the graphs in Figure 20 must be borne in mind in the ensuing discussion of techniques for the measurement of electron parameters. The simplest Langmuir probe, yet the most difficult to analyze, is of the exposed asymmetric type. In the version used by SMITH (1961a, 1961b), the collector is the rocket's nose tip whose surface area is small enough that the rocket potential can be considered the reference potential. The observed collector current as a function of the collector-to-rocket potential (ϕ_{cr}) taken at an altitude of 115 km for a daytime condition is illustrated in Figure 20a. One needs to know the behavior of only the

incoming electron current to compute electron density and temperature. This requires an assumption as to the behavior of the unwanted ion and photocurrents to which the collector also is sensitive. The usual method is to assume that the current observed at high negative potentials is entirely due to i_+ and i_p and by extrapolation subtract their total behavior. The corrected curve illustrated in Figure 20b then is plotted logarithmically and electron temperature is computed from the slope in the exponential regime. For this particular set of data, the reported electron temperature was 1500°K , a value considerably higher than was obtained under quiet solar conditions

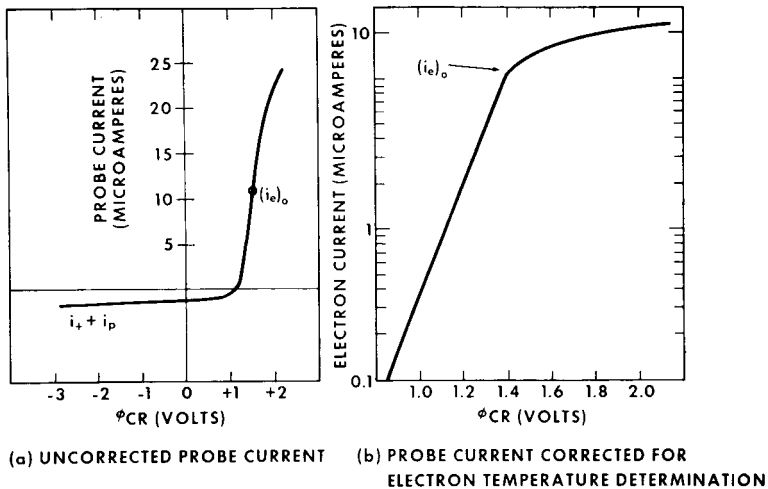


Fig. 20. Typical volt-ampere curves (SMITH, 1961a) from a flush-mounted asymmetric Langmuir probe.

for the same altitude but by different devices (AONO *et al.*, 1961; BRACE, 1962). The difference could be geophysical in nature since the data reported by SMITH (1961a) were obtained within twenty-four hours of a geomagnetic disturbance. However, it also is possible that the variance is attributable to the different techniques used.

It can be seen that the slope of the curve shown in Figure 20b is very sensitive to the assumed i_+ and i_p corrections. Arguments can be made that the effect on electron temperature determination still should be small because i_+ and i_p vary quite slowly with ϕ_{cr} whenever the collector is negative with respect to the plasma potential. The latter point is identified in Figure 20a as the value of ϕ_{cr} where the collector current has the value $(i_e)_0$. The assumption of a slowly varying i_+ and i_p is likely to be correct for probes extended away from a large rocket body. However, for the flush-mounted asymmetric probe used to obtain the data shown in Figure 20, there is a small possibility of current exchange between the collector and the adjacent rocket surfaces. Evidence for such a possibility exists in the form of the shift of the overall curve from the origin, a bias which SMITH attributes to dissimilar collector and rocket surfaces. It is possible, by reason of this bias, that some of the rapid change in collector current

near $(i_e)_o$ is due to unexpected large variations in the unwanted ion or photocurrents and that this could be reflected as an error in the electron temperature determination. The possibility of such errors can only be suggested, not verified at this time.

It should be emphasized that these considerations do not affect significantly the electron density values reported by SMITH and used in Figure 7 to illustrate the diurnal variation of the E region. Again referring to Figure 20, electron density is computed from the measured value of $(i_e)_o$ according to

$$(i_e)_o = (e N_e \bar{c}_e A) / 4, \quad (7)$$

where \bar{c}_e is the mean electron velocity which in turn is proportional to $T_e^{1/2}$. It is seen from Figure 20 that the value of $(i_e)_o$ is some ten times the observed total effect of the unwanted ion and photocurrents. It follows that the electron density determination should be insensitive to the methods used in correcting for i_+ and i_p even though the electron temperature determination is sensitive in this respect. SMITH found that the electron density computed from Equation (7) by insertion of the electron temperature obtained from the exponential slope of the corrected curve is a factor of two higher than that obtained from an ionosonde. This factor could be explained if the slope of the corrected volt-ampere curve and thus the derived electron temperature were in error by a factor of 4. Alternatively, it could be explained by a stronger vehicle velocity effect than expected as was pointed out in the discussions accompanying Figure 19. In either event, since normalization to the ionosonde data did take place the only real error in question is the shape of the electron density profile. If, instead of the assumption of an isothermal electron temperature used by SMITH in deriving the daytime profile shown in Figure 7, one were to assume an electron temperature behavior similar to that of the neutral gas then the errors in the profile would only be about 20 percent. Similarly, the nighttime electron density results should be approximately correct. Consequently, although the electron temperature results obtained from the flush asymmetric probe are subject to some question, the important findings of SMITH relative to the diurnal variation of E region electron densities are not significantly altered by these considerations.

It should be emphasized that the suggestion that asymmetric probes flush-mounted on a rocket could be subject to errors in electron temperature do not necessarily apply to other Langmuir probes that have been flown on spacecraft. As far as the electron temperature parameter is concerned the resonance probe of AONO *et al.* (1961) is in principle an asymmetric Langmuir probe. However, its collector is extended away from the main rocket body which should suppress ion and/or photocurrent exchange between the collector and the main rocket body and additionally should make the results insensitive to perturbations of the ion sheath surrounding the main body. Similarly, confidence can be placed that these types of errors are suppressed in the ejectable asymmetric Langmuir probe used by SPENCER *et al.* (1962) especially since care has been taken in providing appropriate guard rings. It must be noted, however, that the latter two devices measure electron temperature when the collector is negative with respect to plasma potential. For this reason, these probes could contain errors

if there existed the unlikely possibility that the electron energy distribution is not Maxwellian. The only other criticism that can be made of these devices is associated with the time taken to obtain the respective volt-ampere curves. When this time is long, there is a possibility that the electron current is varying with vehicle velocity or magnetic field modulation (as shown in bottom graph of Figure 19) rather than entirely because of the application of the retarding potential. When the electron current varies with probe orientation rather than probe potential, errors in electron temperature can result. Because of the possibility of this particular type of effect, it is considered by this author that the significant changes in electron temperature over small altitude intervals reported by SPENCER *et al.* (1961) are likely not to be real. However, the errors in the overall smoothed altitude curves which SPENCER *et al.* produced by statistical averaging should be small, a conclusion applicable to the results of BRACE (1962) used in Figures 15 and 16.

The electron temperature data used in Figure 17 were reported by SERBU *et al.* (1961) who used a gridded device on the Explorer VIII satellite. By the use of grids, unwanted ion and photocurrents were separated out experimentally permitting unambiguous measurement of the wanted electron current. Additionally, volt-ampere curves were obtained for small changes in vehicle orientation. On the other hand, the use of grids introduces a source of second order errors – that due to changes in the electrical transparency of the grids with retarding potential. The device used by WILLMORE *et al.* (1962) to obtain the data shown in Figure 18 is an exposed probe with appropriate guard ring extended on a boom. The transmission of the first and second derivative of the volt-ampere curves should make for electron temperature determination over extremely short intervals of time and for all pertinent values of probe-to-plasma potential. These features should permit the investigators to report data insensitive to errors due to orientation-induced changes in unwanted ion and photocurrents.

References

- AONO, Y., HIRAO, K. and MIYAZAKI, S.: 1961, *J. Rad. Res. Lab., Japan* **8**, 453.
 BOURDEAU, R. E., DONLEY, L. J., SERBU, G. P. and WHIPPLE, E. C.: 1961, *J. Astron. Sci.* **8**, 65.
 BRACE, L. H.: 1962, Univ. of Mich. Scient. Rept. JS 3, 03599–11–F.
 DONLEY, J. L.: 1963, *J. Geophys. Res.*, April.
 GRINGAUZ, K. I. and ZELIKMAN, M. Kh.: 1957, *Uspehi Fiz. Nauk* **63**, 239.
 HALE, L. C.: 1961, *J. Geophys. Res.* **66**, 1554.
 HANSON, W. B. and MCKIBBIN, D. C.: 1961, *J. Geophys. Res.* **66**, 1667.
 SERBU, G. P., BOURDEAU, R. E. and DONLEY, J. L.: 1961, *Journ. Geophys. Res.* **66**, 4313.
 SHARP, G. W., HANSON, W. B. and MCKIBBIN, D. D.: 1962, *Journ. Geophys. Res.* **67**, 1375.
 SMITH, L. G.: 1961a, AGU Meeting, Washington, D.C., April.
 SMITH, L. G.: 1961b, AGU Meeting, Los Angeles, California, December 27.
 SPENCER, N. W., BRACE, L. H. and CARIGNAN, G. R.: 1962, *J. Geophys. Res.* **67**, 157.
 ULWICK, J. C. and PFISTER, W.: 1961, Am. Astron. Soc. Symposium, 17 March.
 WHALE, H. A.: 1963, *J. Geophys. Res.* **68**, 415.
 WHIPPLE, E. C.: 1959, *Proc. I.R.E.* **47**, 2023.
 WILLMORE, A. C., BOYD, R. L. F. and BOWEN, S. J.: 1962, Conference on the Ionosphere, London, July.